AGU PUBLICATIONS

Tectonics

RESEARCH ARTICLE
10.1002/2016TC004262

**Key Points:**
- The Gulf of Cadiz links shortening across Africa-Iberia boundary from the Atlantic to the Betics
- Four main south directed thrusts responsible for uplift of SW Iberia in the Cenozoic are documented
- Cenozoic thrusting overprints and inverts the Mesozoic passive margin structures

**Correspondence to:**
A. Ramos,
adriaramos@ub.edu;
adria_ramos@outlook.com

**Citation:**
Ramos, A., O. Fernández, P. Terrinha, and J. A. Muñoz (2017), Neogene to recent contraction and basin inversion along the Nubia-Iberia boundary in SW Iberia, *Tectonics*, *36*, 257–286, doi:10.1002/2016TC004262.

Received 4 JUN 2016
Accepted 23 JAN 2017
Accepted article online 25 JAN 2017
Published online 11 FEB 2017



# Neogene to recent contraction and basin inversion along the Nubia-Iberia boundary in SW Iberia

**Adrià Ramos[1], Oscar Fernández[2], Pedro Terrinha[3], and Josep Anton Muñoz[1]**

[1]Institut de Recerca Geomodels, Departament de Dinámica de la Terra i de l'Oceá, Facultat de Ciéncies de la Terra, Universitat de Barcelona, Barcelona, Spain, [2]Dirección de Geociencias, Repsol Exploración, Madrid, Spain, [3]Divisão de Geologia e Georecursos Marinhos, Instituto Português do Mar e da Atmosfera, Lisboa, Portugal

**Abstract** The SW of Iberia is currently undergoing compression related to the convergence between Nubia and Iberia. Multiple compressive structures, and their related seismic activity, have been documented along the diffuse Nubia-Iberia plate boundary, including the Gorringe bank west of the Gulf of Cadiz, and the Betic-Rif orogen to the east. Despite seismic activity indicating a dominant compressive stress along the Algarve margin in the Gulf of Cadiz, the structures at the origin of this seismicity remain elusive. This paper documents the contractional structures that provide linkage across the Gulf of Cadiz and play a major role in defining the present-day seismicity and bathymetry of this area. The structures described in this paper caused the Neogene inversion of the Jurassic oblique passive margin that formed between the central Atlantic and the Ligurian Tethys. This example of a partially inverted margin provides insights into the factors that condition the inversion of passive margins.

## 1. Introduction

Since the end of the Mesozoic, the Iberian microplate has been trapped between the converging African and Eurasian plates [*Dewey et al*., 1989; *Rosenbaum et al*., 2002]. As a consequence, the paleogeographic and tectonic evolution of Iberia as well as their surrounding margins during the Cenozoic have been strongly linked to the Alpine orogeny and to the closing of the Tethys Ocean [e.g., *Ziegler*, 1988; *Dewey et al*., 1989]. Cenozoic N-S convergence between Africa and Eurasia is thus the cause of the development of a number of mountain chains in the internal parts of the Iberian microplate and along its northern and southern margins (the Pyrenean-Cantabrian chain, the Spanish Central System, the Sierra Morena, and the Betic-Rif chain; Figure 1b) [*De Vicente et al*., 2004; *Vergés and Fernàndez*, 2012]. These mountain chains are interpreted to represent the westernmost termination of the Alpine-Himalayan orogenic system [*Dewey et al*., 1973; *Şengör*, 1984; *Dercourt et al*., 1986].

From the Late Cretaceous and throughout the Cenozoic, deformation in Iberia migrated from north to south, as the Iberian microplate progressively welded with the Eurasian plate. Orogenic deformation in the Iberian plate initiated along the Pyrenean-Cantabrian chain along its northern border in Late Cretaceous. By the early Miocene, orogenic deformation, and the Nubia-Iberia boundary, had migrated to the south of Iberia, to the Betic-Rif system [*Srivastava et al*., 1990a, 1990b]. West of Iberia, the Azores-Gibraltar Fracture Zone (AGFZ), and its eastern continuation along the Southwest Iberian Margin lineaments [*Zitellini et al*., 2009] in the southern Gulf of Cadiz, is interpreted as the current Nubia-Iberia plate boundary in the Atlantic Ocean (Figure 1a) by some authors [e.g., *Maldonado et al*., 1999; *Zitellini et al*., 2009].

The present-day Nubia-Iberia plate boundary between the AGFZ and the Gibraltar Arc (the link between the Rif and Betic orogens) has been described as a diffuse plate boundary by *Sartori et al*. [1994]. The transition from the AGFZ, which originates as a transform in the mid-Atlantic, into the contractional systems of Iberia has been the subject of study in recent years [e.g., *Maldonado et al*., 1999; *Zitellini et al*., 2009]. This has led to the identification of multiple contractional features with neotectonic activity (and potential tsunamigenic hazard) at the eastern termination of the AGFZ immediately west of the Gulf of Cadiz, namely, the Gorringe Thrust, Horseshoe Thrust, Marquês de Pombal Thrust, and the Coral Patch Ridge (Figure 1) [*Gràcia et al*., 2003a; *Terrinha et al*., 2003; *Zitellini et al*., 2004; *Jiménez-Munt et al*., 2010; *Sallarès et al*., 2013, *Martínez-Loriente et al*., 2014, 2016].

Previous structural interpretations of the Gulf of Cadiz have concentrated on the Algarve Basin as part of the SW Iberian passive margin [e.g., *Terrinha*, 1998; *Matias et al*., 2011]. Thus, the structures responsible for the seismic activity and Neogene deformation in the Gulf of Cadiz remained elusive [*Carrilho et al*., 2004]. In

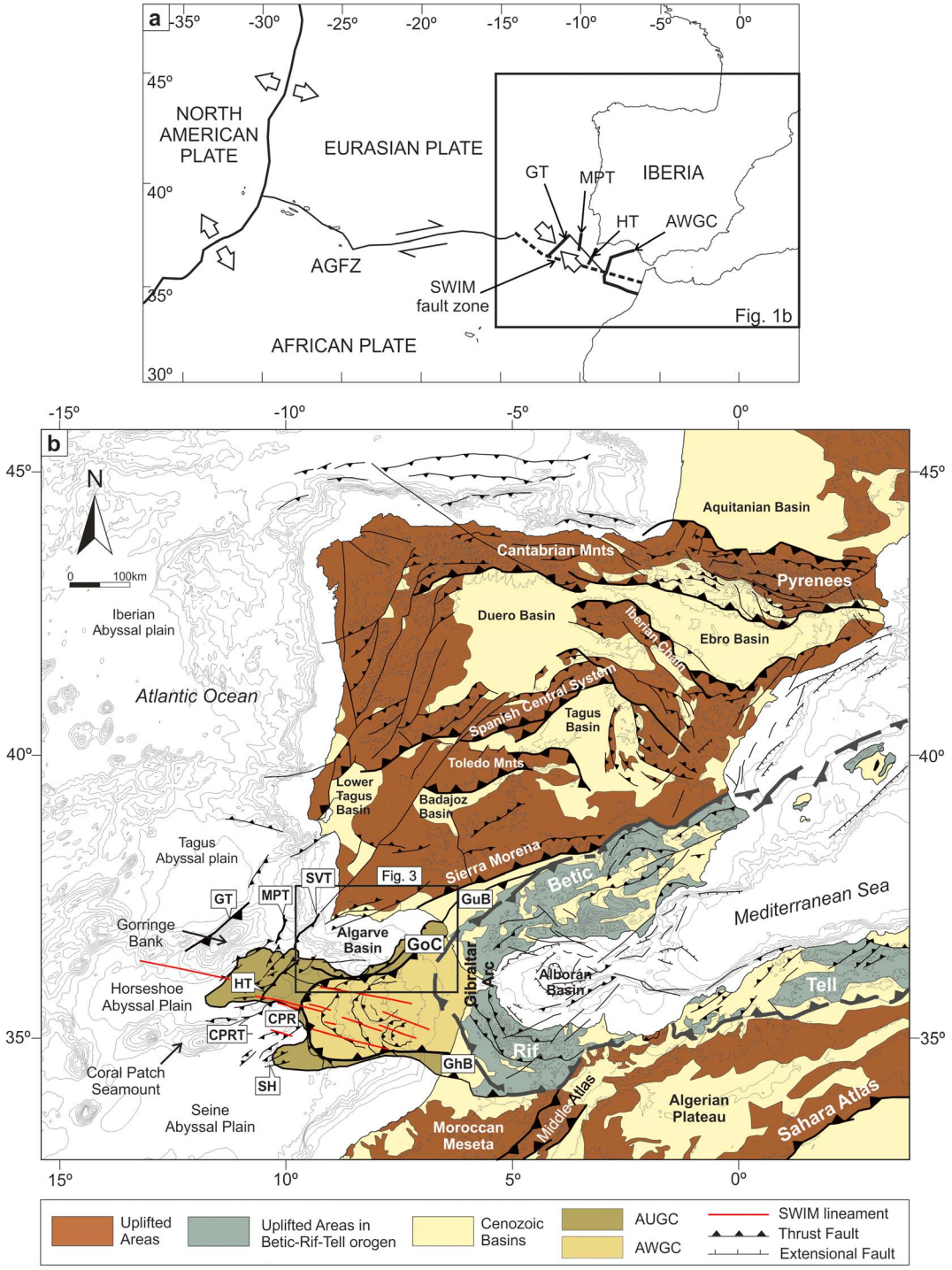


**Figure 1.** (a) Main elements of plate boundaries and relative plate kinematics. (b) Map showing the location of Cenozoic contractional structures in Iberia and surrounding areas related to the Nubia-Iberia plate boundary. AGFZ: Azores-Gibraltar Fracture Zone, AUGC: Allochthonous Unit of the Gulf of Cadiz, AWGC: Allochthonous Wedge of the Gulf of Cadiz, CPR: Coral Patch Ridge, CPRT: Coral Patch Ridge Thrust, GuB: Guadalquivir Basin, GhB: Gharb Basin, GoC: Gulf of Cadiz, GT: Gorringe Thrust, HT: Horseshoe Thrust, MPT: Marquês de Pombal Thrust, SH: Seine Hills, SVT: São Vicente Thrust. Adapted using data from *Gomez et al.* [2000], *Michard et al.* [2008], *De Vicente and Vegas* [2009], *Gutscher et al.* [2009], *Medialdea et al.* [2009], *Zitellini et al.* [2009], *De Vicente and Muñoz-Martín* [2013], *Duarte et al.* [2013], and *Martínez-Loriente et al.* [2013].

this paper we aim to document the contractional structures that link the AGFZ and the Gibraltar Arc across the Algarve Basin and are the locus of major instrumental seismic activity. We will demonstrate that these features are, at least in part, responsible for the deformation and uplift of the SW Iberian margin from Oligocene to present.

The partial inversion of passive margins, similar to that documented here for the SW Iberian margin, is a common feature to the western and northern Iberian margins [*Peron-Pinvidic et al*., 2008; *Duarte et al*., 2013; *Tugend et al*., 2014; *Druet*, 2016]. Partial inversion has also been documented in other parts of the Tethyan domain [e.g., *Gardosh and Druckman*, 2006; *Arsenikos et al*., 2013] and the North Atlantic [e.g., *Boldreel and Andersen*, 1993; *Vågnes et al*., 1998; *Lundin and Doré*, 2002; *Johnson et al*., 2005; *Doré et al*., 2008]. The inversion of oblique to transform margins has even been explored in areas such as the Svalbard-West Barents margin of Norway [e.g., *Faleide et al*., 2008; *Indrevær et al*., 2016], the Otway Basin of Australia [*Hill et al*., 1994], or the Santos Basin of Brazil [*Cobbold et al*., 2001]. In recent years there have been an increasing interest in the geological evolution of passive margins, mainly since new concepts on hyperextended margins were proposed [*Peron-Pinvidic and Manatschal*, 2009; *Brune et al*., 2016]. As a result, the influence of the rift inheritance, particularly the distribution of the different rifts domains and the rift architecture, has been proposed to play a significant role on margin inversion and subsequent continental collision [*Roca et al*., 2011; *Tugend et al*., 2014]. However, a problem arises when considering the relative role that other factors may have contributed to the compressional deformation of margins other than the rift inheritance, such as prerift inheritance or obliquity of the deformation axis during the subsequent tectonic events.

Within this context, the example presented here of the SW Iberian margin provides key insight into the elements that control the initial stages of inversion of a passive margin. In particular, inherited heterogeneities at different scale and of different nature appear to be the main controlling factor in the configuration of the inverted margin. We will propose that the pattern of inversion observed in this margin is the consequence of crustal heterogeneities inherited from the (prerifting) Paleozoic Variscan orogeny, the structure of the rifted margin, and its Mesozoic mechanical stratigraphy.

## 2. Geological Setting

### 2.1. Tectonic and Geodynamic History of the Algarve Margin Since the Mesozoic

The evolution of southern Iberia during the Mesozoic was dominated by rifting associated to the westward propagation of the Tethys and to the opening of central and North Atlantic [*Handy et al*., 2010; *Schettino and Turco*, 2011]. The southern margin of Iberia developed during this time as a transtensional rift margin connecting the central Atlantic with the Ligurian Tethys [*Handy et al*., 2010]. Rifting of southern Iberia led to the development of a thick Mesozoic sequence of sediments in fault-controlled depocenters unconformably overlying a Paleozoic basement. Mesozoic extension in the Algarve Basin was dominated by the development of roughly E-W trending extensional faults and the presence of NW-SE trending transfer zones or faults [*Terrinha*, 1998; *Ramos et al*., 2016].

The Algarve Basin is the only remnant of the southern Iberian rift margin that was not overprinted by the Betic orogenic system in the Cenozoic. At the time of the opening of the North Atlantic in the Early Cretaceous, Iberia was an isolated microplate, separated from Eurasia by the Bay of Biscay-Pyrenean rift system and from Africa by a transcurrent oceanic ridge-transform system [*Sallarès et al*., 2011].

Evolution of southern Iberia since Late Cretaceous has been dominated by the convergence between Africa and Eurasia and the progressive southward migration of deformation and orogeny across the Iberian plate previously discussed. Deformation in the Late Cretaceous to Cenozoic intraplate mountain chains of Iberia is deep rooted, involving basement and, where present, inverting preexisting Mesozoic rift basins. In addition to the generation of intraplate relief, the relative motion of Africa, Iberia-Eurasia, and the western Mediterranean also led to the development of the Betic-Rif orogen from late Oligocene to middle Miocene [*Lonergan and White*, 1997].

### 2.2. Stratigraphy

The Algarve Basin started to develop during the Triassic, with the deposition of siliciclastic continental sediments unconformably overlying the Carboniferous flysch deformed in the foreland of the Variscan foreland and infilling roughly E-W trending half-grabens [*Terrinha*, 1998; *Ramos et al*., 2016] (Figure 2). Triassic

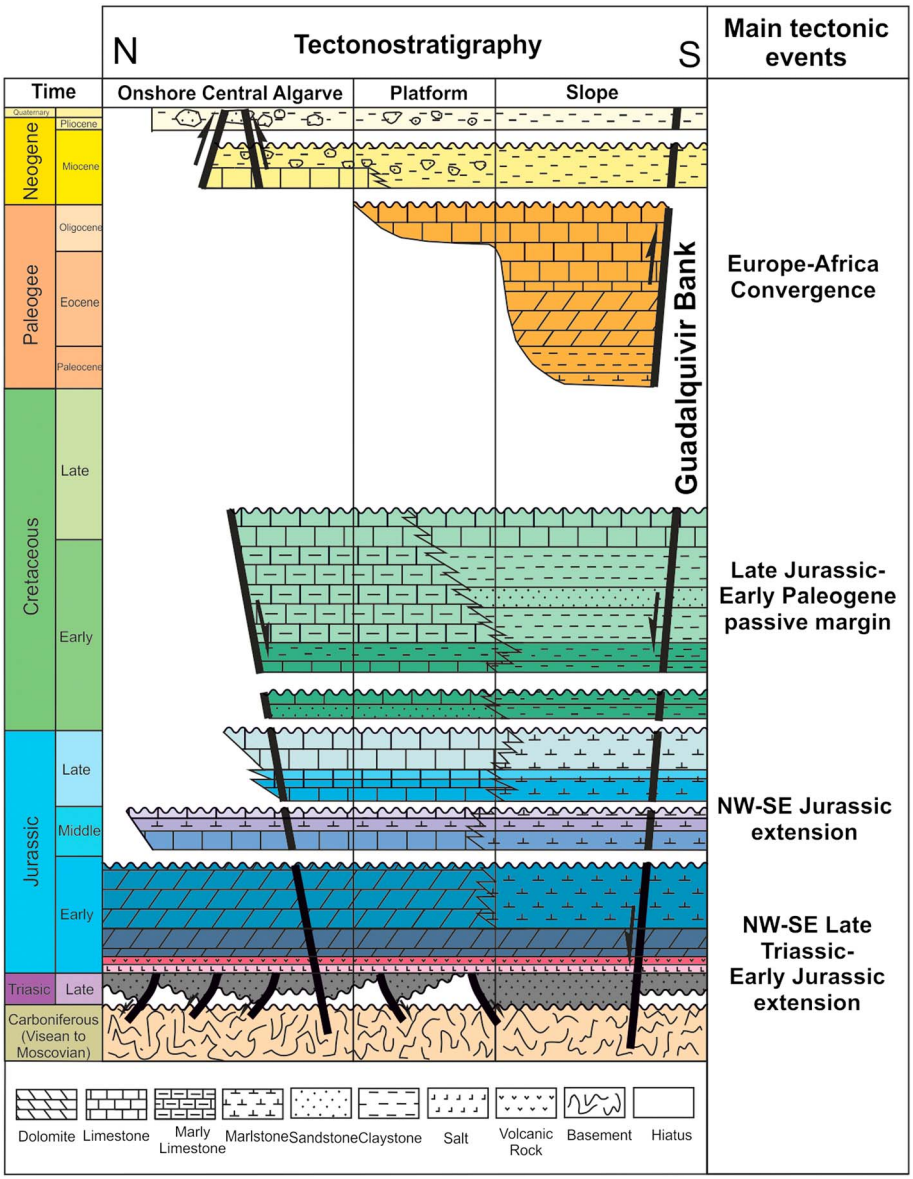


**Figure 2.** Synthetic stratigraphy of the Algarve Basin with the main tectonic events and the seismic character for each stratigraphic unit interpreted in this work.

sediments are covered by Hettangian evaporites and terrigenous clastics (Figure 2), which are capped in turn by a volcanic-sedimentary complex, Hettangian-Sinemurian in age, and associated with the central Atlantic Magmatic Province [e.g., *Martins et al*., 2008]. During a period of Sinemurian tectonic quiescence, shallow water limestones and dolomites were deposited in the basin (Figure 2). From Pliensbachian to Toarcian (at the transition to the Middle Jurassic), the basin recorded progressive deepening with the development of marly facies with abundant ammonoid fauna [*Terrinha et al*., 2002].

Extensional and salt tectonics controlled the basin configuration during the Middle and Late Jurassic, affecting sediment distribution and thickness. During this time, deposition was dominated by carbonates [*Terrinha*, 1998; *Ramos et al*., 2016] (Figure 2). An allochthonous salt body (the Esperança Salt) sourced from the lowermost Lower Jurassic (Hettangian) evaporite layer was emplaced progressively from mid-Jurassic up to Miocene times in the eastern half of the Algarve Basin [*Matias*, 2007].

The Lower Cretaceous, represented by siliciclastics and carbonates (Figure 2), shows variations in thickness related to the ongoing salt tectonism and locally to basement-involved extensional faulting. Overall,

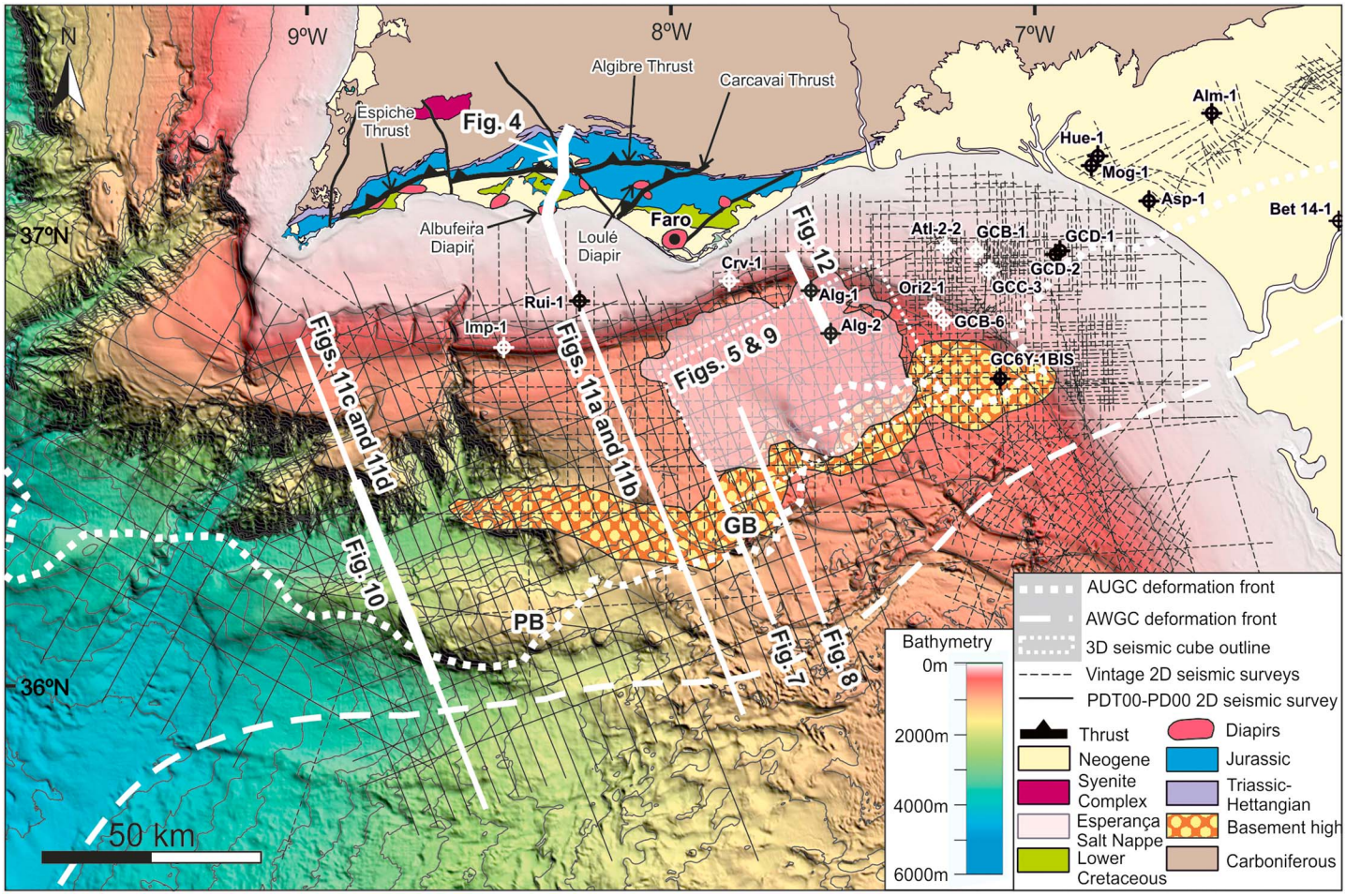


**Figure 3.** Map showing the available data in the SW Iberian margin with bathymetry colored for depth and the location of the figures described below in this paper. GB: Guadalquivir Bank, PB: Portimão Bank. High-resolution bathymetry is taken from the General Bathymetric Chart of Oceans (GEBCO) digital atlas [*IOC et al.*, 2003]. The most representative wells are also depicted in this figure as follows: Alg-1: Algarve-1, Alg-2: Algarve-2, Alm-1: Almonte-1, Asp-1: Asperillo-1, Atl-2-2: Atlantida-2-2, Bet 14-1: Betica 14-1, Crv-1: Corvina-1, GCB-1: Gulf of Cadiz B-1, GCB-6: Gulf of CadizB-6, GCD-1: Gulf of CadizD-1, GCD-2: Gulf of CadizD-2, GCD-2: Gulf of CadizC-3, GC 6Y-1Bis: Gulf of Cadiz6Y-1Bis, Hue-1: Huelva-1, Imp-1: Imperador-1, Mog-1: Moguer-1, Ori 2-1: Orion 2-1, Rui-1: Ruivo-1. See Figure 1b for the location.

Cretaceous sediments reflect a shallowing of the basin and a reduction in accommodation space. The Lower Cretaceous sediments are followed by a very condensed Upper Cretaceous succession or an equivalent sedimentary hiatus and/or an angular unconformity at the base of the Paleogene, reflecting regional uplift during this time. The Paleogene is partially preserved in the offshore, represented by shallow water carbonates (Figure 2). Above the Paleogene, Miocene deposits overlie the Basal Foredeep Unconformity (BFU) (Figure 2 [*Ledesma*, 2000; *Maldonado et al.*, 1999]) and are a mix of siliciclastics and carbonates in the proximal areas of the basin and turbidite-dominated clastics in the deeper parts. The BFU is a key marker as it records Miocene and younger deformation.

Finally, the Pliocene-Quaternary succession consists of siliciclastics (Figure 2). Pliocene to Present sedimentation in the Gulf of Cadiz is controlled by the Mediterranean Outflow Water (MOW), whose activity started with the opening of the Strait of Gibraltar in Pliocene times [*Hernández-Molina et al.*, 2014]. This current resulted in the deposition of fine-grained contourite drifts, strongly controlling the present-day seafloor geometry.

### 2.3. Shortening Structures

To date, the contractional deformation and basin inversion experienced elsewhere in Iberia have only been documented to affect the Algarve Basin to a small extent as mostly isolated features in the onshore and the offshore.

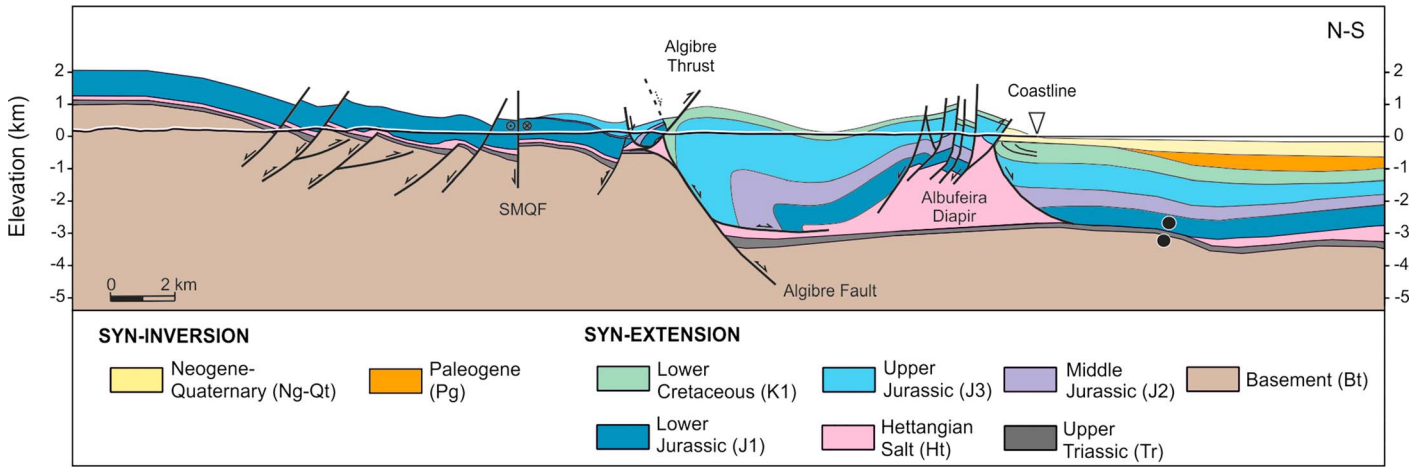


**Figure 4.** Cross section along the onshore central Algarve Basin. Extensional motion on the southward dipping Algibre fault from Jurassic to Cretaceous times was responsible for the formation of the rollover structure, later inverted during Cenozoic compression. Inversion also led to the formation shortcuts and inversion of extensional faults in the northern sector of the figure. Notice the Algibre Thrust detaching on the Hettangian evaporite unit in the footwall of the Algibre fault. Modified after *Ramos et al*. [2016]. See Figure 3 for the location.

#### 2.3.1. Onshore Structures

Contractional structures are mainly observed along the northern margin of the basin, which crops out due to approximately 350 m of Plio-Pleistocene uplift of southern Portugal [*Feio*, 1951; *Dias and Cabral*, 1997; *Terrinha*, 1998]. This uplift causes southward tilting of the Paleozoic basement and the overlying Mesozoic along the northern outcrop limit of the Algarve Basin (Figure 4). Dips of Mesozoic beds are as high as 32° toward the south and form a continuous monocline along the entire northern outcrop margin of the Algarve Basin. This southward tilt of beds has led to the presence of a clear break in topography, such that the basin is flanked to the north by a sudden rise of topographic relief in the order of up to 200 m (Figure 4). In addition to the regional southward tilt, the basin margin is also characterized by south directed shortcut structures that developed in the footwall of E-W trending extensional faults that bound Triassic half-grabens (Figure 4) [*Terrinha*, 1998; *Ramos et al*., 2016].

Further basinward, the Algibre Thrust (Figures 3 and 4), described by *Manuppella* [1992] and *Terrinha* [1998], is a laterally continuous E-W trending, southward directed thrust that can be correlated to the west with the Espiche Thrust [*Ramos et al*., 2016] (Figure 3). The Algibre Thrust detaches on the regionally ubiquitous Early Jurassic evaporite level [*Ramos et al*., 2016] (Figure 4). In its footwall, Mesozoic beds are characterized by multiple E-W trending tight folds, produced by buttressing against a southward dipping Mesozoic extensional fault (Figure 4) [*Ramos et al*., 2016]. Age for the Algibre thrust cannot be constrained precisely, but the youngest materials in its footwall are Early Cretaceous in age.

Throughout the onshore portion of the basin, isolated salt structures also record shortening and reactivation. The Loulé Salt diapir (Figure 3) displays various pulses of shortening, associated to progressive exhumation of the diapir [*Terrinha et al*., 1990]. The Albufeira Diapir (Figures 3 and 4) also shows two phases of contractional deformation [*Terrinha et al*., 2013; *Ramos et al*., 2016], attested by the deformed and thrusted Miocene overlying isoclinal folds of the Lower Cretaceous.

#### 2.3.2. Offshore Structures

In the offshore, the Portimão Bank (Figure 3) was documented by *Roque* [2007] and *Terrinha et al*. [2009] to be a Mesozoic graben inverted from Neogene times to present day. To the east of the Portimão Bank, the Guadalquivir Bank (Figure 3) is a prominent bathymetric high, but its precise nature has remained elusive. Other than the Portimão Bank, no contractional structures have been documented within the offshore Algarve Basin.

The most evident Cenozoic contractional feature in the Gulf of Cadiz lies to the south of the Algarve Basin but provides key timing relationships discussed in this paper. It is a giant chaotic unit emplaced synchronously with the development of the Betic-Rif orogen. This chaotic unit is divided into two subunits: one of tectonic origin and a second one related to gravitational collapse of the first one. The first one is the Accretionary

Wedge of the Gulf of Cadiz (AWGC), also labeled GCIW, Gulf of Cadiz Imbricated Wedge, by some authors), and the second one is the Allochthonous Unit of the Gulf of Cadiz (AUGC), labeled HGU, Horseshow Gravitational Unit, by some authors) [*Torelli et al*., 1997; *Iribarren et al*., 2007]. The Accretionary Wedge of the Gulf of Cadiz (AWGC) consists of a thick chaotic, mélange-like assemblage of Mesozoic to Cenozoic rocks affected by west migrating thrust system. The AWGC developed as the outermost structure of the Betic-Rif orogen during the Miocene as the orogenic arc progressed westward driven by the roll back of the Gibraltar subducted oceanic slab [*Gutscher et al*., 2002]. Disagreement exists as to the ongoing activity of the accretionary wedge [*Gutscher et al*., 2002, 2009; *Medialdea et al*., 2004; *Iribarren et al*., 2007]. The AUGC is an olistostrome, gravitationally emplaced submarine debris flows sourced from the AWGC [*Iribarren et al*., 2007; *Gutscher et al*., 2009]. It buried the front of the AWGC along the entire front of the Betic and Rif, over the Guadalquivir and Gharb forelands and their extension toward offshore. To the west, the lack of a shallow continental mass allowed the AUGC to spread downslope into the deep ocean [*Torelli et al*., 1997]. Locally, the AUGC is seen to be incorporated into the accretionary wedge [*Thiebot and Gutscher*, 2006]. There is general agreement that the AUGC was emplaced by Late Tortonian [*Perconig*, 1962; *Torelli et al*., 1997; *Tortella et al*., 1997; *Flinch and Vail*, 1998; *Maldonado et al*., 1999]. It overlies a regional unconformity that defines the base of the Betic foredeep deposits (BFU) [*Maldonado et al*., 1999; *Ledesma*, 2000].

### 2.4. Present-Day Configuration

The Mesozoic to Cenozoic Algarve Basin sits between the Atlantic oceanic thrusts (Gorringe, Marquês de Pombal, and Horseshoe Thrusts) and the Betic-Rif orogen (Figure 1b), areas of known Miocene to present contractional deformation. This area is dominated at present day by transpressional to compressional stress due to its location relative to the plate boundary between the Nubian and Iberian plates [*Zitellini et al*., 2009; *DeMets et al*., 2010]. The Algarve Basin, and the broader Gulf of Cadiz, has been documented as a tectonically active domain by many authors [*Gràcia et al*., 2003a, 2003b; *Duarte et al*., 2009, 2010; *Terrinha et al*., 2009; *Zitellini et al*., 2009; *Duarte*, 2011; *Martínez-Loriente et al*., 2013, 2014]. Seismicity, as indicated by focal mechanisms, is coherent with N-S to NW-SE directed shortening across the Gulf of Cadiz [*Zitellini et al*., 2009; *Palano et al*., 2013; *Custódio et al*., 2015, 2016]. The Guadalquivir and Portimão Banks, which define the southern boundary of the Algarve Basin (Figure 3), have been identified as tectonically active features since the Neogene [*Ribeiro et al*., 1979; *Mougenot*, 1989; *Terrinha*, 1998; *Gràcia et al*., 2003a; *Zitellini et al*., 2004; *Terrinha et al*., 2009].

## 3. Data and Methods

The observations and interpretation of the structure of SW Iberia and the Algarve Basin presented in this paper are based on interpretation of seismic data, well data, geological mapping of onshore Portugal, and gravity and magnetic data. Data have been integrated with regional geological understanding to ensure that the interpretation is coherent with the history of Mesozoic extension and Cenozoic compression experienced by SW Iberia.

Vintage 2-D seismic surveys of the Gulf of Cadiz and a more recent 2-D regional seismic reflection survey (acquired by TGS in 2001 during the PDT00 and PD000 cruises [*TGS*, 2005]) have been used to interpret the offshore structure in the Gulf of Cadiz (Figure 3). The PDT00-PD00 regional survey consists of a set of 58 lines of 2-D multichannel reflection seismic data. This seismic survey consists of NNW-SSE lines spaced every 4 km and ENE-WSW lines spaced every 8 km, and it has a shot point interval of 12.5 and 15 m. Recording length was 12 s two-way travel time (TWTT). The interpretation on this survey was performed on the migrated stack in time.

A 3-D seismic cube was acquired in 2012 by Repsol in the central part of the offshore margin, from south of Faro to the Portuguese-Spanish border (Figure 3). It covers an area of 1500 $km^2$ and it consists of 151 shot lines oriented NNW-SSE and spaced every 375 m, with a recording length of 7.2 s TWTT. This 3-D cube has also been interpreted, using the prestack time and prestack depth migrated versions.

Seismic interpretation was constrained by the calibration with 5 wells in offshore Portugal [*Roque*, 2007] along with 67 wells in the Gulf of Cadiz and Guadalquivir Basin [*Lanaja*, 1987] (the location of the most relevant wells is shown in Figure 3). Portuguese wells have been tied to seismic using their individual check shot data or average interval velocities (Figure 2) when check shot data was of poor quality or not available. The interval velocities have been calibrated using the depth image of the depth-migrated 3-D seismic cube to

make it meaningful for the deeper portions of the basin where no wells are available. Seismic profiles have been interpreted using Petrel (by Schlumberger). Conversion of 2-D seismic profiles to depth has been performed where necessary using Move 2014.2 (by Midland Valley Exploration).

Seismic correlation has been based on the interpretation of unconformity-bounded sequences [*Terrinha*, 1998; *Roque*, 2007]. The seismic response is different in every stratigraphic unit. Paleozoic is represented by transparent and chaotic seismic facies, sometimes stratified (e.g., Figure 8). The basement is followed by the first Mesozoic sediments, the Triassic, represented by middle-to-high-frequency and high-amplitude reflectors (e.g., Figure 9). The roof of this section coincides with the base of the Hettangian evaporites, describing a strong reflector (Figure 9). Evaporite seismic facies are made of chaotic and transparent reflectors. Salt tectonic structures are typically represented by positive and irregular strong reflectors, deforming the overlying and surrounding sediments (Figure 8). The seismic image shows a poor quality beneath salt structures (Figure 10).

Lower Jurassic shows low-frequency and high-amplitude reflectors (e.g., Figure 5). Middle and Upper Jurassic show similar seismic response (e.g., Figures 5 and 9) and present some unconformities, such as the Bajocian-Bathonian and the Callovian-Oxfordian among the most representative. The Lower Cretaceous, represented by middle-to-high-frequency and medium-amplitude reflectors, tends to onlap the Upper Jurassic (e.g., Figure 5). The Upper Cretaceous and the Paleogene, where present, lay over an erosional unconformity over the last unit. They are represented by strong middle-amplitude and middle-frequency reflectors (e.g., Figure 6). Neogene and Quaternary are depicted by high-frequency and low-amplitude continuous reflectors, and onlap the BFU, while its roof represented the seafloor (e.g., Figure 6).

The AUGC is depicted by a highly irregular roof and an erosional flat base, with chaotic and transparent internal facies (e.g., Figure 6). The AWGC has a similar seismic response, although the southward dipping reflectors suggest the presence of imbricated thrusting (Figure 10) [*Gutscher et al*., 2002]. To the south and southeast the image beneath is obscured by both bodies (AUGC and AWGC).

Seismic interpretation has also been integrated with published onshore data [*Ramos et al*., 2016]. Finally, gravity and magnetic modeling [*Ramos et al*., 2015] have been used to constrain the deeper seismic horizons (pre-Jurassic picks, mainly the top of basement) and the crustal-scale structure.

## 4. Contractional Structures of the Algarve Basin

The preservation of the overall Mesozoic age rift architecture of the Algarve Basin gives a false impression that the basin has not experienced major inversion and merely subsided in the Cenozoic as the foredeep to the Betic-Rif orogen. In this section we aim to demonstrate that contractional structures of Cenozoic age are more common in the area than previously documented. To do this we will provide an overview of known and newly documented contractional structures, from the onshore basin margin to the offshore.

Multiple scales of contractional deformation features in the offshore Algarve Basin can be observed on 2-D and 3-D reflection seismic data. On one hand, there are thrusts detaching within the Mesozoic sediments that can be clearly identified on seismic activity, and their activity dated is based on stratigraphic unconformities. On the other hand, there are angular relationships and observations which cannot be tied down to specific structures visible on seismic but can be ascribed to basement-involving structures, possibly thick-skinned blind thrusts.

### 4.1.1. Reactivated Salt Structures in the Eastern Algarve Basin

The contractional structures most evident on seismic in the offshore Algarve Basin are those associated with the deformation of salt bodies, mainly in the allochthonous Esperança Salt (Figures 3 and 5), which shows squeezing of salt structures in its central part (Figure 5). Salt accumulations related with the salt structures that formed during the rifting stage of the Algarve Basin were the weakest parts of the basin and the areas prone to localize and record the subsequent contractional deformation.

In the central part of the profile of Figure 5, an antiform cored by imbricated Lower Cretaceous and Jurassic sediments can be observed (Figures 5 and 6). Structural relief related with this contractional structure is of 1.7 km. Unfolding of the top of Cretaceous to a restored geometry (Figure 5c) indicates that shortening on this structure was in the order of 2.5 km. Onlap of the Paleogene onto the Lower Cretaceous and the thinning of Quaternary sediments over this structure demonstrate that this antiform grew from Paleogene until recent

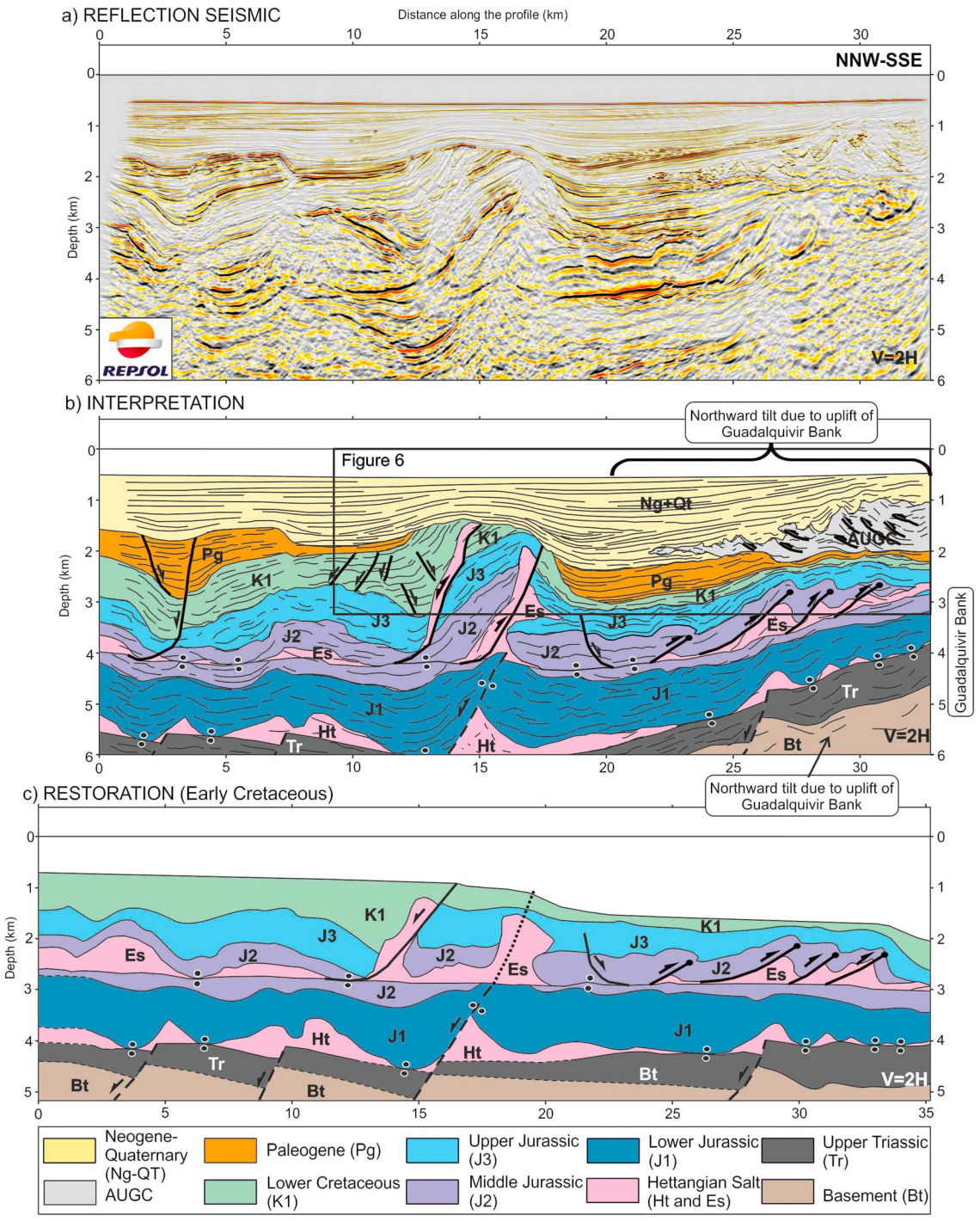


**Figure 5.** Seismic section across the Esperança Salt. (a) Reflection seismic profile (extracted from a proprietary 3-D seismic cube migrated in depth). (b) Interpretation of Figure 5a. (c) Restoration at Early Cretaceous time. Black dashed line: inferred fault and horizon, Ht: autochthonous evaporitic layer, Es: Esperança Salt. The section is a NNW-SSE trending section through the 3-D seismic survey shown in Figure 3 (the precise location is not shown due to confidentiality). Data courtesy of Repsol.

times. Different stages of growing are emphasized by the three main unconformities observed in the growth package (Figure 6). Paleogene sediments onlap the Lower Cretaceous unit on the southern limb of the antiform, evidencing the earliest stages of folding. Above, the BFU unconformity truncates the imbricated Jurassic to Paleogene sediments in the core of the antiform, revealing a period of more intense shortening and erosion. It is worth noting that the BFU connects with the basal surface of the AUGC (Figure 6), demonstrating the synchronicity between antiformal growing and the emplacement of the AUGC.

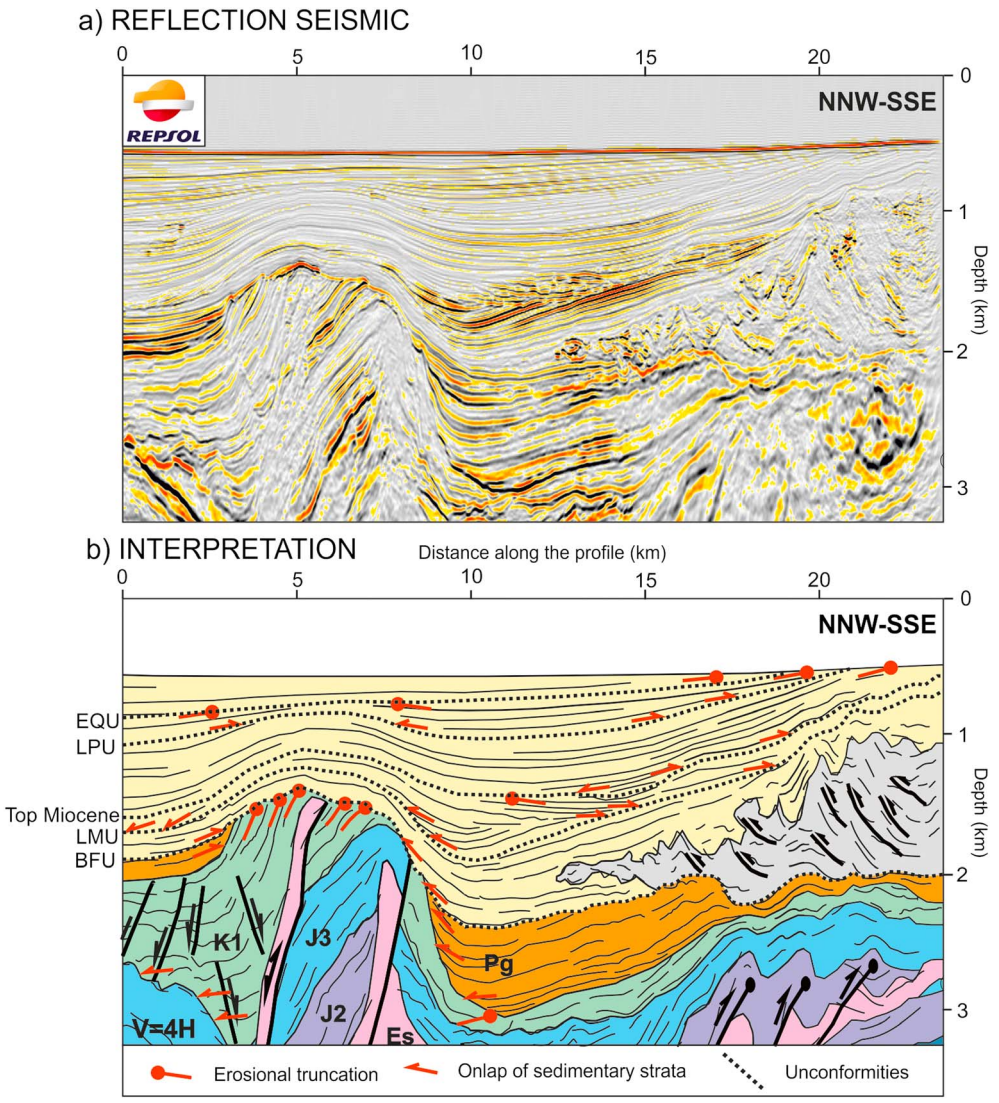


**Figure 6.** (a) Seismic section of the detailed Cenozoic unit over the Esperança Salt in Figure 5b. (b) Seismic interpretation showing the main unconformities within the Cenozoic sediments described by *Hernández-Molina et al.* [2016], along with the onlaps and erosional truncations resulting from different tectonic pulses. See Figure 5 for the legend. BFU = Basal Foredeep Unconformity, LMU = Late Miocene Unconformity, LPU = Late Pliocene Unconformity, EQU = Early Quaternary Unconformity.

The AUGC is sandwiched between its basal contact and an unconformity within the late Miocene (labeled LMU on Figure 6), which truncates Miocene growth sediments and is folded by the antiform (Figure 6). Above the LMU, a highly reflective wedge-shaped set of reflectors could correspond to contourite deposits related with the circulation of Mediterranean Outflow Water from the Gibraltar strait to the Gulf of Cadiz since Pliocene times [*Llave et al.*, 2011], channeled between the AUGC and the Guadalquivir Bank and the growing antiform. These sediments, as well as the younger succession above, show a growth geometry at both sides of the anticline. They also have experience a regional northward tilting and moderate deformation by the reactivation of the internal structures of the AUGC (Figure 6). Despite Pliocene sediments being dominated by contouritic deposits, onlap onto the late Pliocene unconformity [*Hernández-Molina et al.*, 2016] and truncation below the Early Quaternary Unconformity [*Hernández-Molina et al.*, 2016] observed in this section are interpreted to respond to tectonic causes and not primary sedimentary geometry [see also *Hernández-Molina et al.*, 2016]. The symmetrical arrangement of the Pliocene-Quaternary sedimentary growth wedges at both sides of the antiform demonstrates the progressive tilting of their limbs. This geometry significantly differs from the wedge-shaped contourite drifts deposited in the adjacent structural lows (Figure 6). Contourite

deposits are dominated by sheeted drifts and mostly constant thickness other than around tectonically active structures [*Hernández-Molina et al*., 2016].

The internal structure of the antiform consists of two thrusts involving the Jurassic and Lower Cretaceous sediments. However, normal throw of the Jurassic across the northern thrust and the presence of a localized, thick Upper Jurassic/Lower Cretaceous depocenter strongly affected by extensional faults demonstrate extensional faulting, downbuilding, and salt evacuation, indicating the existence of a salt wall that has been subsequently squeezed to form a thrust weld. The southern thrust would also correspond to a thrust weld formed by shortening of a salt wall (Figure 5c). This salt wall could correspond to a feeder connecting the autochthonous Hettangian Salt horizon with the allochthonous Esperança Salt nappe. The reconstructed geometry of the section in Figure 5 at Early Cretaceous time (Figure 5c) shows that none of the salt walls accommodated any shortening prior to the Late Cretaceous.

The section in Figure 5 also contains two other sets of contractional features. For one, Figure 5c shows a set of shortening structures already present at Early Cretaceous times along the southern end of the section. These are part of a south directed fold-and-thrust system detached on the allochthonous Esperança Salt. This system is interpreted to be the toe-thrust system associated to the allochthonous emplacement and gravitationally driven deformation of the Esperança Salt in Middle to Late Jurassic times. Folds and thrusts record syntectonic thinning and thickening of Middle to Upper Jurassic sediments, defining a pre-Cretaceous age for the thrusting. Folding of overlying units is interpreted to relate to a later reactivation.

The last set of contractional features observed on this section (Figure 5) is related to the AUGC. The base of the AUGC is seen to tectonically erode Paleogene sediments and climb up stratigraphically toward the north. The chaotic facies of this body are in response to highly deformed sediments due to intense thrusting and sedimentary reworking during transport. The top of this body is highly irregular due to postemplacement mobilization of sediments, probably driven by shale tectonism (documented by the abundant shale diapirs in the Gulf of Cadiz) [*Medialdea et al*., 2009]. The resulting minibasins are infilled by late Miocene sediments.

#### 4.1.2. Guadalquivir Bank

The Guadalquivir Bank is an elongated ENE-WSE seamount 50 km long and 30 km wide (Figure 3) constituted by a core of Paleozoic basement that locally crops out at the seafloor as testified by dredging [*Malod and Mougenot*, 1979; *Gràcia et al*., 2003a, 2003b]. To the SW, this bathymetric high links with another positive bathymetric structure, the Portimão Bank (Figure 3).

Figure 5 ends short of the crest of the Guadalquivir Bank (note outline of 3-D seismic survey in Figure 3). The basement that can be seen on the southern end of the section rising up toward the south is the northern flank of the Guadalquivir Bank. Just as the basement is tilted to the north, overlying Mesozoic and Cenozoic sediments (ranging from Paleogene to Quaternary, including the base of the AUGC) are dipping to the north. Within the Cenozoic package, late Miocene to late Pliocene age sediments that onlap and blanket the AUGC are dipping north and truncated at the seabed above the Guadalquivir Bank (above the AUGC at the right end of the section; Figure 6). These sediments are in turn onlapped by sediments of latest Pliocene to Quaternary age (Figure 6), which are truncated by the seabed and are the same sediments involved in the antiform resulting from the reactivation of salt walls in the center of the section (Figure 6).

The northward dip of Mesozoic to Cenozoic sediments on the northern limb of the Guadalquivir Bank is observed also on 2-D seismic lines (Figures 7–9 and 11). It is also associated to truncation of the most recent sediments at the seabed observed in the Figures 6 and 9 and by contouritic moats in Figures 7 and 8. Likewise, erosion associated to the BFU is seen to locally remove the entire Paleogene and truncate the top of the Lower Cretaceous over the Guadalquivir Bank (Figures 8 and 9) before being draped by Miocene sediments. As in the case of Figure 6, late Pliocene sediments are clearly tilted and erosionally truncated at the seabed above the Guadalquivir Bank in the sections in Figures 8b and 9b. Quaternary sediments are also observed to onlap tilted Pliocene sediments in Figure 8b. All these geometries are clear indications of uplift of the Guadalquivir Bank from Paleogene to Present, in at least two distinct stages: a late Paleogene (or early Miocene?) stage, accounting for the erosional truncation below the BFU, and a late Pliocene to Quaternary stage that accounts for tilting and truncation at the seabed of late Pliocene and older sediments.

Paleogene or early Miocene uplift of the Guadalquivir Bank explains why the bank acted as a barrier to the progression during the middle to late Miocene of the AUGC in its southern flank (Figures 3, 7, 8, and 11). The AUGC was only capable of overcoming this physiographical barrier locally (e.g., Figure 5) in areas of

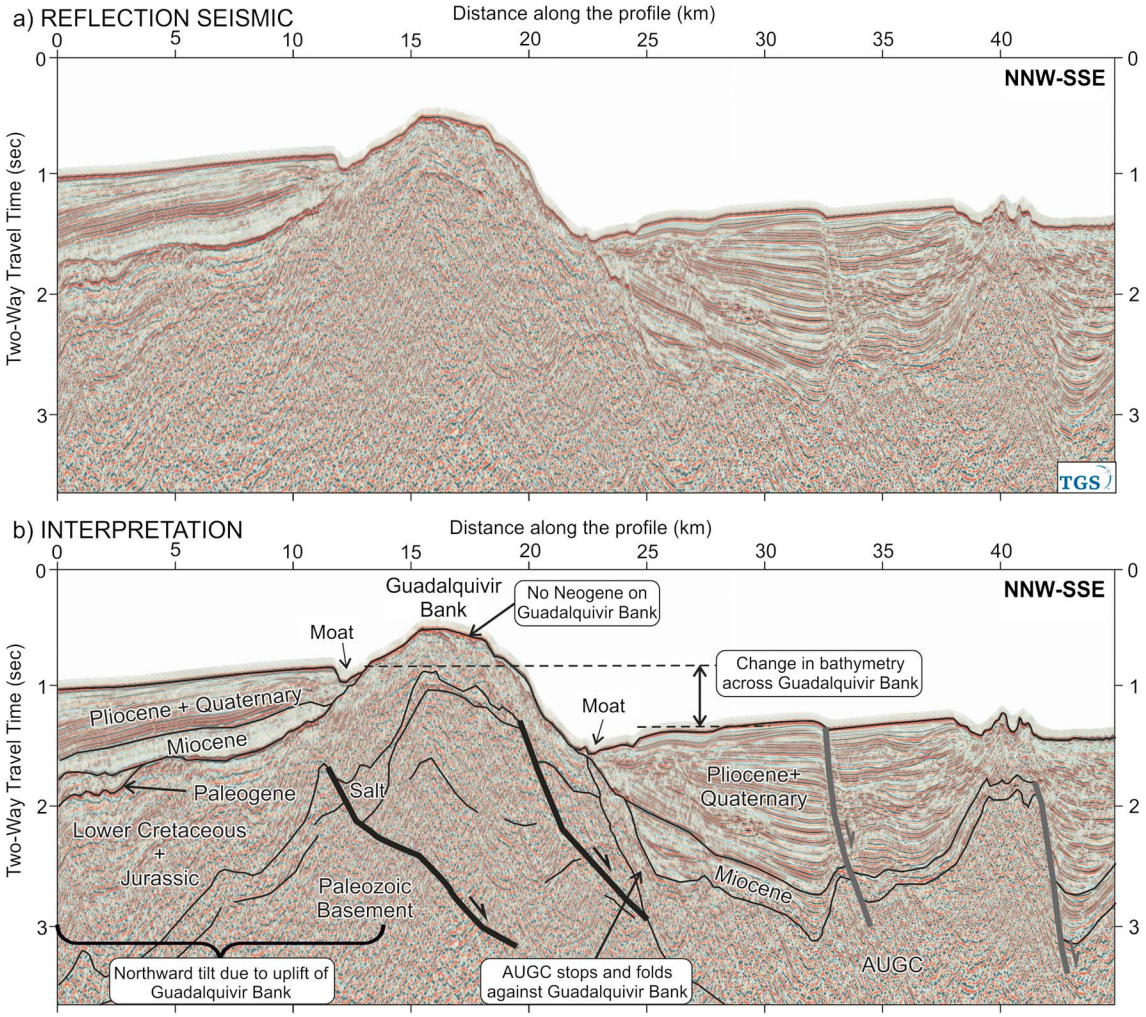


**Figure 7.** (a) Seismic section across the Guadalquivir Bank in TWTT and (b) its interpretation. Note the bathymetric relief of the Guadalquivir Bank and its lack of inner reflectivity. The onlap of Miocene to Quaternary sediments on both flanks indicates the presence of pre-Miocene sediments at seabed on the Guadalquivir Bank. Note also the northward tilt of sediments on the north of the Bank and the southward steepening of the AUGC and Miocene sediments on the south. See Figure 3 for the location. Data courtesy of TGS.

lesser uplift of the bank. Recent uplift also accounts for the noticeable drop in bathymetry (in the order of 200–400 m) that occurs across the bank (Figures 7 and 8) and that conditions present-day sea bottom contouritic currents (MOW) and erosion (note the localization of contouritic moats on both flanks of the bank in Figure 7 and on the southern flank of the Bank in Figure 8).

The 3-D seismic cube reveals the presence of north directed thrusts in the northern flank of the Guadalquivir Bank, affecting the sediments ranging from basement to Early Cretaceous (Figure 9). These are interpreted as back thrusts accommodating part of the contractional deformation due to the uplift of the Guadalquivir Bank by the basal regional thrust. In some cases, based on the thickening of pre-Cretaceous sediments in their hanging wall, they seem to reactivate previous Triassic-Jurassic extensional faults.

Beyond the geometries that are related to Cenozoic shortening and uplift, some geometries observed on the seismic profiles already discussed prove the relevance of the Guadalquivir Bank as a structural high during basin extension in the Mesozoic. The section in Figure 8, for instance, shows that the basement high under the Guadalquivir Bank can be interpreted as the footwall of a major extensional fault dipping toward the south/southeast. In this case, the hanging wall of the extensional fault has been uplifted by approximately 2 km by Cenozoic thrusting (see Figures 8c and 8d) and deeply eroded by the BFU before being "onlapped" by the AUGC and later sediments. The equivalent Mesozoic in the footwall of the thrust responsible for uplift

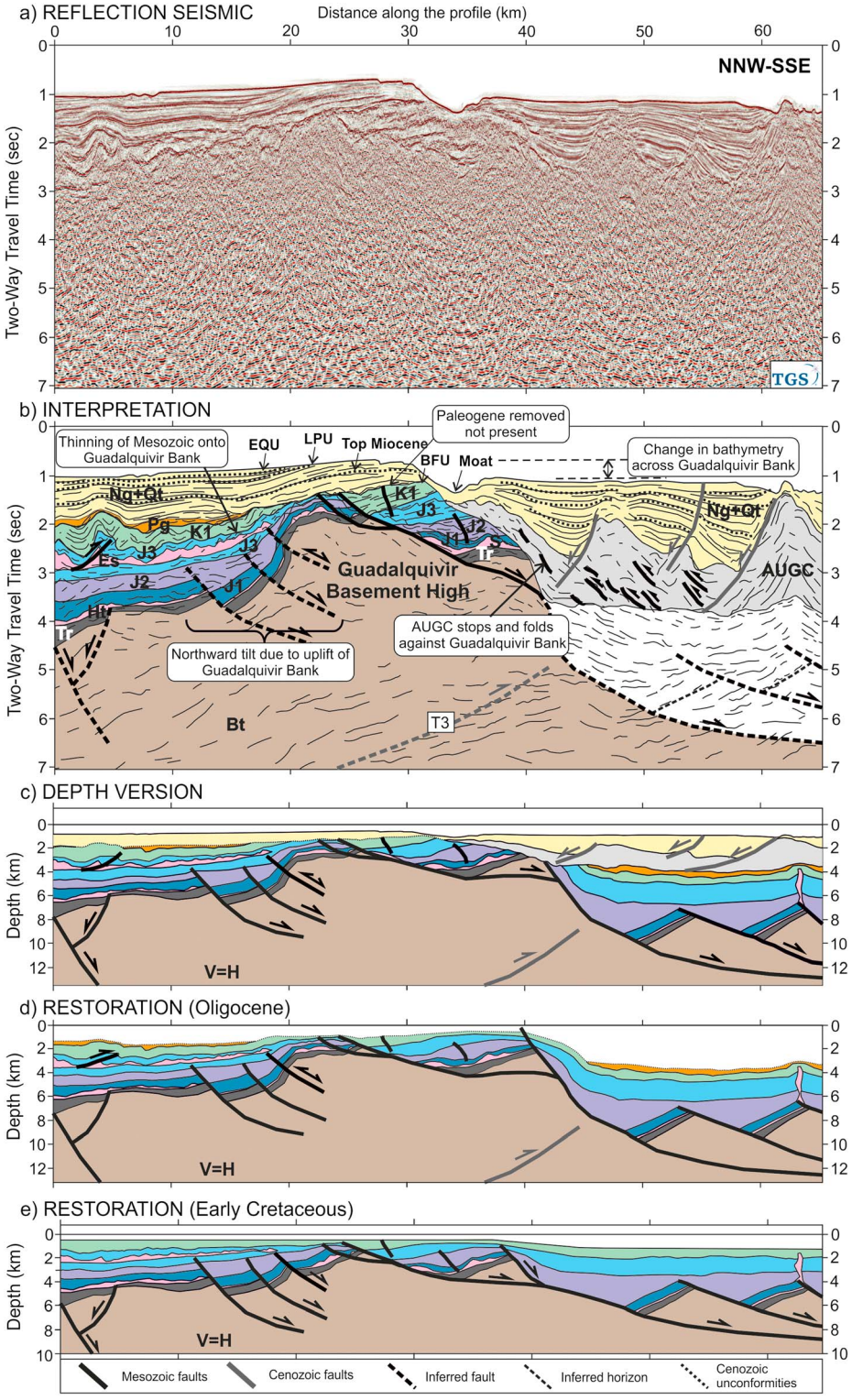


**Figure 8.** Seismic section across the Guadalquivir Bank. (a) Reflection seismic profile in time. (b) Interpretation of the same profile. (c) Depth version of profile in Figure 8a. (d) Restoration at Oligocene time (prior to the emplacement of the AUGC). (e) Restoration at Early Cretaceous time. The interpretation beneath the depth of 3–4 s is based on the 3-D seismic image north of the Guadalquivir Bank and inferred to its south due to the poor seismic image. Extensional faults interpreted north of the Guadalquivir Bank are projected from 3-D seismic interpretation (see Figure 9). See Figure 3 for the location and Figure 5 for the legend. BFU = Basal Foredeep Unconformity, LPU = Late Pliocene Unconformity, EQU = Early Quaternary Unconformity. Data courtesy of TGS.

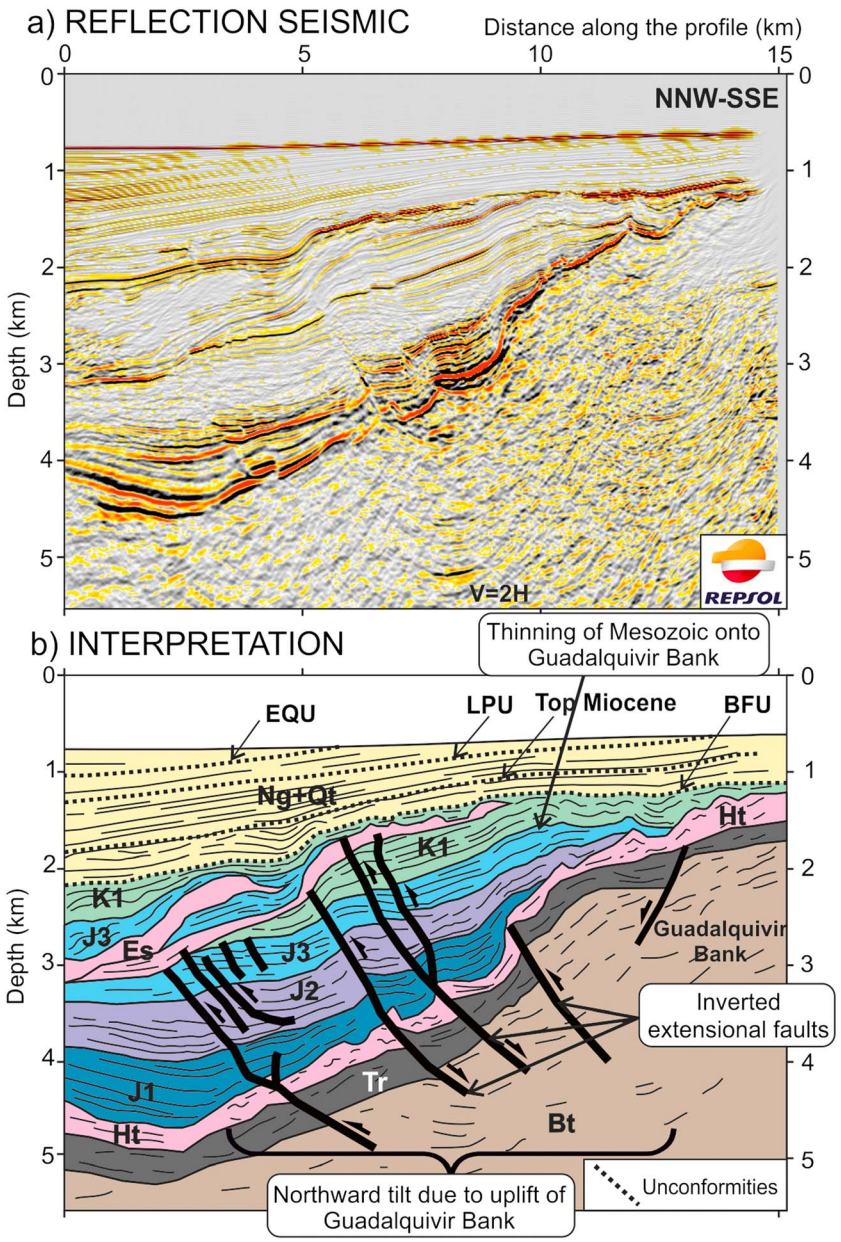


**Figure 9.** (a) Reflection seismic profile in depth across the northern flank of the Guadalquivir Bank and the southwestern portion of the Esperança Salt and (b) its corresponding interpretation. See Figure 5 for the legend. The section is the southern portion of a NNW-SSE trending section through the 3-D seismic survey shown in Figure 3 (the precise location is not shown due to confidentiality). BFU = Basal Foredeep Unconformity, LPU = Late Pliocene Unconformity, EQU = Early Quaternary Unconformity. Data courtesy of Repsol.

of the bank is interpreted to be in the order of 4 to 6 km deeper than that in the hanging wall of the thrust (the base of the AUGC that is assumed to lie over Paleogene and Mesozoic sediments, as in Figure 5, is at a depth of nearly 4 km). This difference in depth of Mesozoic sediments across the Guadalquivir Bank can also be seen on other sections through the area (e.g., Figures 7 and 11b if the Mesozoic south of the bank is also inferred to lie under the base of the AUGC). It is difficult to account for this throw merely by Cenozoic uplift; we interpret that Mesozoic extensional faulting predating thrusting can account for part of this vertical offset (Figures 8d and 8e).

The relationship of the Guadalquivir Bank basement high with Mesozoic sediments to the north is not as clear on seismic due to poor image quality. Locally, where image is good enough, onlap and thinning of

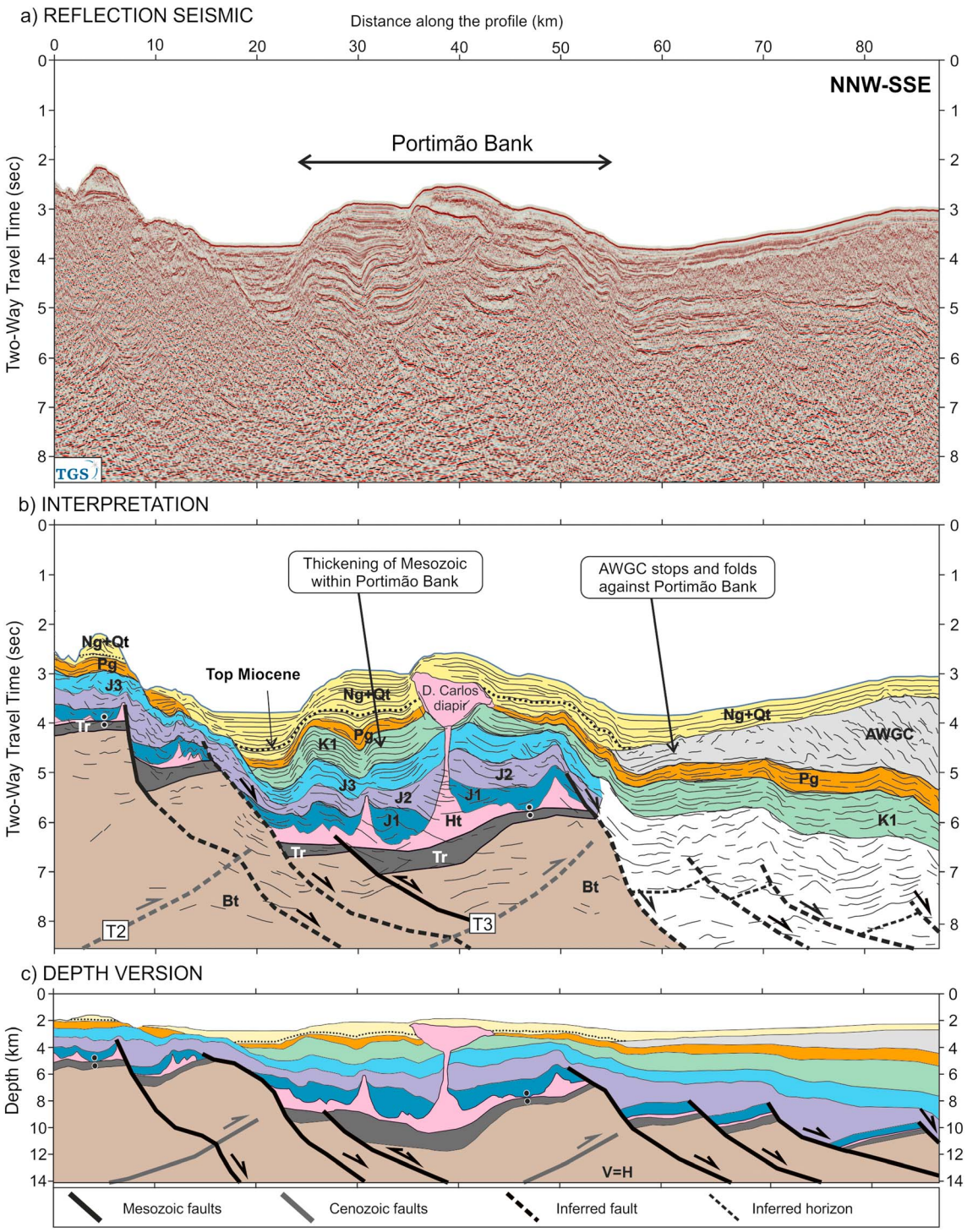


**Figure 10.** Representative section across the Portimão Bank. (a) Reflection seismic profile in time. (b) Interpretation of the profile in Figure 10a. (c) Depth version of the profile. See Figure 3 for the location and Figure 5 for the legend. The interpretation of the deep section south of the Portimão Bank is inferred. Data courtesy of TGS.

Cretaceous and Jurassic sediments onto the basement high can be seen, inferred to represent infill of a basin flanking a basement high (Figure 8e). In other cases, progressive depositional thinning of the Jurassic and Lower Cretaceous sediments toward the Guadalquivir Bank (Figures 5 and 9) indicate that the basement under the Guadalquivir Bank was already dipping gently to the north prior to Cenozoic deformation. This is consistent with the interpretation of the Guadalquivir Banks as a basement high during Mesozoic

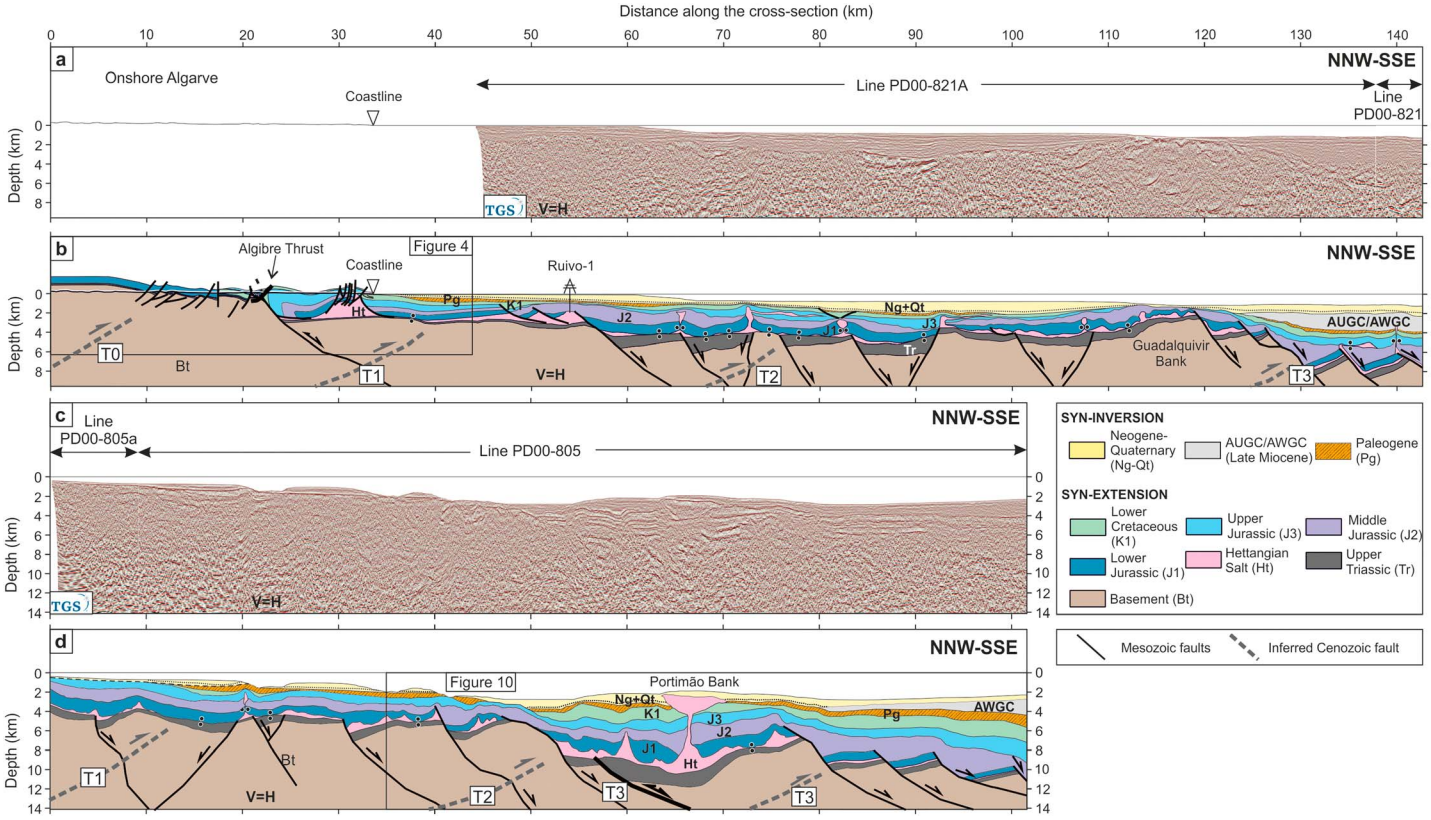


**Figure 11.** Cross sections through the Algarve Basin showing the major contractional structures identified. (a) Composite seismic section through the central Algarve Basin. (b) Interpretation of the seismic in Figure 11a, with interpretation extended onshore and complemented with outcrop data. (c) Seismic section through the western Algarve Basin. (d) Interpretation of seismic in Figure 11c. The black dots represent the salt welds. See Figure 3 for the location. BFU = Basal Foredeep Unconformity, LPU = Late Pliocene Unconformity, EQU = Early Quaternary Unconformity. Seismic data courtesy of TGS.

extension by previous authors [*Terrinha*, 1998; *Matias*, 2007]. Our observations indicate that the Guadalquivir Bank basement high initially originated as the uplifted footwall of a major (possibly crustal scale) south dipping Mesozoic extensional fault (Figure 7d). This structure was later inverted by a south verging thrust that caused further uplift of the Guadalquivir Bank from Paleogene to Present.

### 4.1.3. Portimão Bank

In contrast to the Guadalquivir Bank, which is a basement-cored structure, the Portimão Bank (Figures 3, 10, and 11d) has been interpreted as an inverted Mesozoic fault-bounded basin by *Terrinha et al*. [2009]. The Mesozoic nature of sediments in the half-graben is supported by the presence of the Dom Carlos diapir (Figure 10), evident on bathymetry as a dome structure, and interpreted to be constituted by Early Jurassic Salt (the only evaporitic unit known in the region) [*Terrinha et al*., 2009]. At the core of the bank, wedging of Mesozoic sediments toward the south and the steeper bathymetry on the northern flank of the bank (Figure 10) indicate that this is an inverted Mesozoic half-graben developed on a south dipping extensional fault. Inversion is of Neogene to recent times, as inferred from the folding of constant-thickness Paleogene strata, thickness variations observed in Miocene and younger sediments, and present-day bathymetry (Figure 10). As with the Guadalquivir Bank, its uplift from late Paleogene or early Miocene times is recorded by the tipping of the AWGC along the southern flank of the bank (Figure 10). To the south, the Mesozoic and Paleogene units beneath the AWGC are deformed in monoclines (Figure 10), suggesting compaction folding over basement rotated blocks. The Neogene-Quaternary sediments and the seabed also show deformation in the Portimão Bank, coherent with the monocline geometry affecting the sediments below (Figure 10), suggesting a recent reactivation for these thrust faults. The continuous growth of the Dom Carlos diapir through Neogene times to present day was probably partly driven by contractional reactivation.

Inversion of the Portimão Bank Mesozoic half-graben is consistent with N-S to NW-SE shortening and with present-day seismic activity that indicates NNW-SSE directed compression [*Dewey et al*., 1989; *Srivastava*

*et al*., 1990b; *Roest and Srivastava*, 1991; *Maldonado et al*., 1999; *Zitellini et al*., 2001, 2009; *Rosenbaum et al*., 2002; *Muñoz-Martín et al*., 2012; *Palano et al*., 2013; *Custódio et al*., 2015]. Faults cannot be traced unambiguously on seismicity, but present-day positive bathymetry and the rapid thickening of Jurassic and Cretaceous sediments into the Portimão Bank cannot be accounted for only by salt tectonics but can be better explained as an inverted Mesozoic fault-bounded graben (Figure 10). Unlike the Guadalquivir Bank, there is no change in the regional level of bathymetry on both sides of the Portimão Bank. Major bathymetric changes occur toward the north of the bank (Figure 10) and are associated with southward steepening of Jurassic sediments and the localization of contouritic moats (Figure 10). To the south of the Portimão Bank there is an increase in depositional space for the Neogene-Quaternary (this space includes the AUGC and the AWGC).

## 5. Discussion

### 5.1. Regional Basement Uplift

Significant Neogene to Recent uplift of the basement along the northern margin of the Algarve Basin has been documented by inspection of the Pliocene marine unconformity [*Feio*, 1951; *Dias and Cabral*, 1997]. Likewise, uplift of the basement at the edge of the southern part of the Algarve Basin (which coincides with the southern limit of SW-Iberia continental crust) is occurring at Present across the Guadalquivir Bank (as discussed above; Figure 7). The uplift of basement at both locations trends WSW-ENE, parallel to the trend of the inherited Mesozoic extensional faults and perpendicular to the dominant direction of present-day convergence between Africa and Eurasia [*Olaiz et al*., 2009; *Pérez-Peña et al*., 2010; *Muñoz-Martín et al*., 2012].

The origin of the basement uplift at these and other locations cannot be identified on seismic or in the field as no major basement thrusts are observed on either. However, there are multiple indications that uplift is being caused by southward verging, deep-rooted blind thrusts. For instance, the uplift observed along the northern margin of the basin is regional, causing an elevated topography to the north. This regional uplift and the southward tilt of Mesozoic units along the basin margin can be consistent with uplift generated by a southward directed contractional structure of crustal scale (along the style of deformation discussed by *Fernández-Lozano* [2012]; between 0 km and 10 km in Figure 11b). This interpretation is also compatible with the interpretation of *Terrinha* [1998] that the tilting at the basin margin is related to broad antiformal folding during the Cenozoic.

Likewise, uplift and tilting of the northern flank of the Guadalquivir Bank extend up to 10 km north of the bank, indicating a deep source for the tilt. Although no thrust responsible for this tilt or uplift has been identified on seismicity, a southward vergent basement involving thrust is the simplest way to account for the gentle northward tilt of beds north of the bank and the steep drop observed to the south. This thrust would be equivalent in nature to that proposed before for the northern outcrop margin of the basin (between 0 km and 10 km in Figure 11b). A southward vergence of thrusting is also supported by the fact that the tilt of the AUGC and Miocene sediments on the southern limb of the bank is much greater than that on the northern limb (Figures 7 and 8). Likewise, Miocene to Recent depositional space (including the space taken by the AUGC, emplaced in the Miocene) south of the bank is considerably greater (2000 m or more).

The northern basin margin and the Guadalquivir Bank are in the order of 100 km apart. Over this distance, the basement must rise from approximately 5 km depth just north of the Guadalquivir Bank to hundreds of meters above sea level along the northern basin margin (Figure 11b). Southward deepening of the basement is consistent with the expected passive margin geometry (deepening oceanward). However, documented Plio-Pleistocene uplift of the basin margin [*Feio*, 1951; *Dias and Cabral*, 1997; *Terrinha*, 1998] along with the geometry of the BFU and overlying Neogene sediments in the offshore indicates that at least part of this difference in depth of the basement is related to Cenozoic deformation. The geometry of the BFU is characterized by deepening southward across relatively rapid steps. At least three of these steps can be identified in outcrop and subsurface.

As has already been discussed, the northernmost step in the BFU occurs across the northern outcrop limit of the basin (Figures 4 and 11). This step in the BFU is related to a relatively narrow southward verging monocline, less than 5 km wide, for which a south directed blind thrust is the most likely culprit.

A similar monocline geometry can be seen locally on some seismic profiles, close the coast. Figure 12, for instance, was shot across one of these monoclines (although incompletely). Basement, which lies at

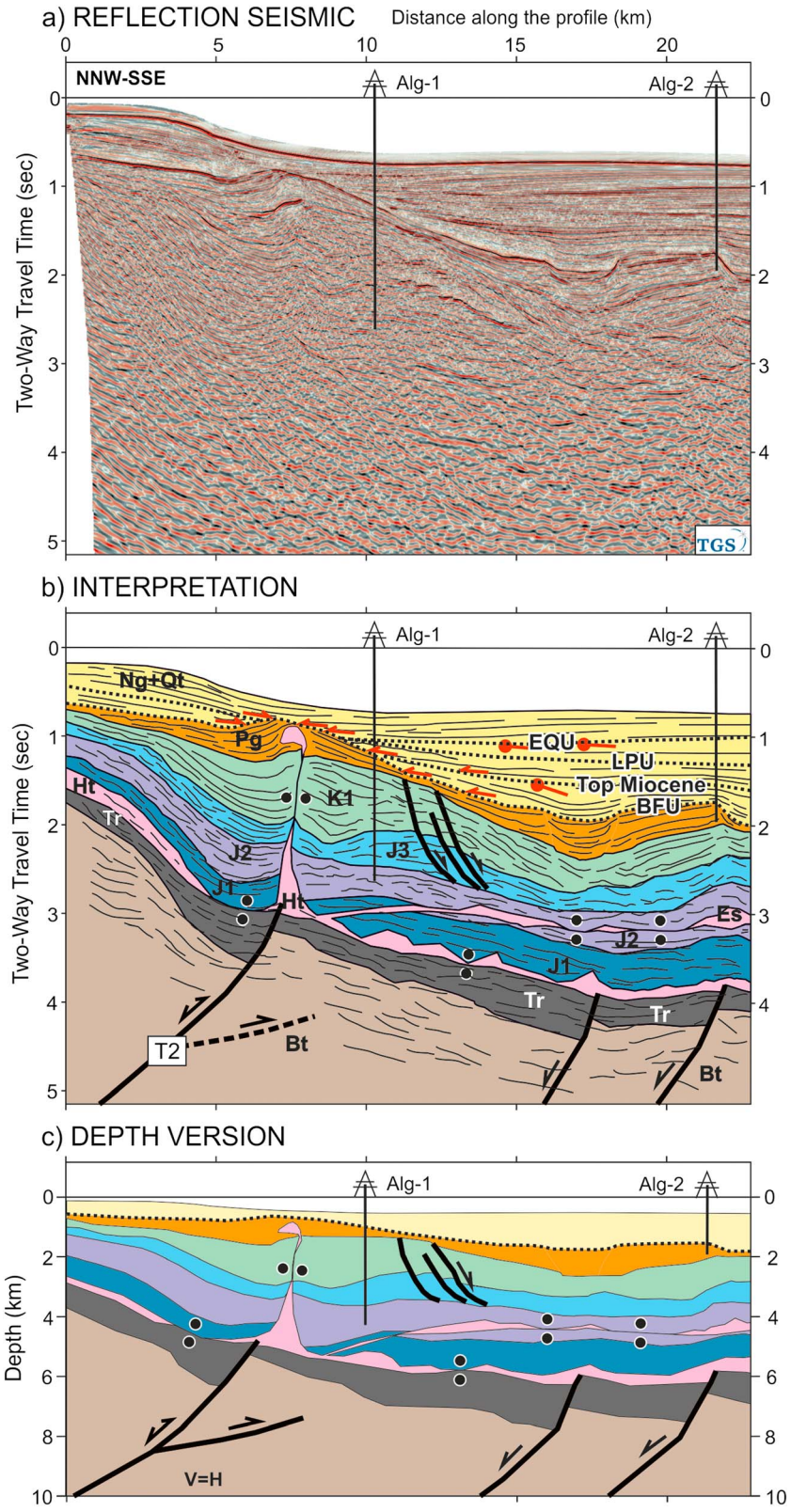


**Figure 12.** Seismic section across the shelf break in the proximal margin of the Algarve Basin and the underlying thrust T2. (a) Reflection seismic profile. (b) Interpretation of the same seismic profile. (c) Depth version of profile in Figure 12b. Black dashed line: inferred fault. See Figure 3 for the location and Figures 5 and 6 for the legend. Data courtesy of TGS.

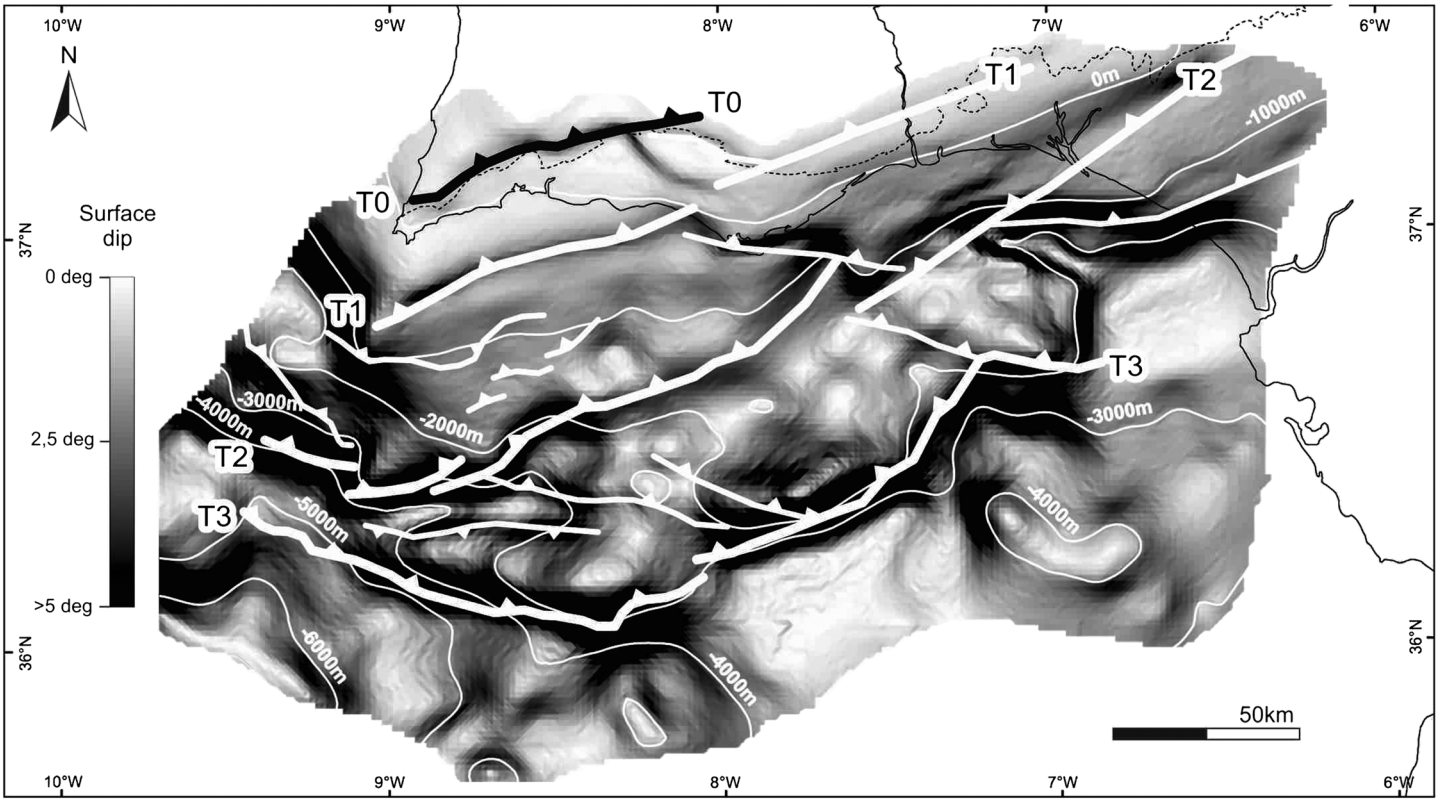


**Figure 13.** Map of the BFU colored for dip, with white contours indicating depth below sea level. Steeper parts of the surface indicate the steps in the surface, interpreted to be related to erosional geometries or to the presence of underlying basement-involving blind thrusts (traces of the thrust tips shown in white lines).

roughly 7 km in depth on the southern end of the image, rises progressively, in a broad monocline, over a distance of approximately 25 km to a depth of around 4 km (an uplift of roughly 3 km). Part of the change in depth of the basement is linked to extension, as can be seen by the thinning of the Mesozoic from 5 km on the south to less than 3 km in the north. This Mesozoic thinning is interpreted to be linked to the configuration of extensional faults and half-grabens. However, not the entire geometry is Mesozoic in origin; of the 3 km of uplift, only 2 km can be accounted for by Mesozoic extension based on the change of thickness of the Mesozoic. The remaining 1 km of uplift is of post-Paleogene times. In Figure 12, the BFU (or top Paleogene) is seen to rise by approximately 1 km from south to north. This uplift is accompanied by a significant northward onlap of Miocene and Pliocene sediments and overall thinning of the Miocene-Quaternary sediments by nearly 1 km. Furthermore, the present-day shelf break (possibly controlled by contourite currents) is located exactly above the step in the basement and slightly offset relative to the step in the BFU, indicating a possible neotectonic control. All these elements indicate that at least 1 km of uplift is accommodated at this location during the Neogene to Present across a step less than 10 km wide.

The Guadalquivir Bank is the location of the third monoclinal step in the basement and in the BFU (Figures 8 and 11b). The Guadalquivir Bank also has a combined origin for the basement high. On one hand, the entire Mesozoic section is seen to thin southward onto the Guadalquivir Bank (Figure 8), indicating that the Guadalquivir Bank was relative high during this time. Above this, Neogene to Quaternary sediments are seen to also thin onto the bank as well as being uplifted and truncated at the seafloor (Figure 8), related to Cenozoic contraction and uplift.

The geometry in these three well-documented locations (the basin outcrop margin, the northern end of Figure 12, and the Guadalquivir Bank) indicates that the uplift of the basement, related to Cenozoic shortening, occurs at discrete locations, few kilometers across, separated by long intervening segments (tens of kilometers) with relatively constant basement depth. Across these narrow areas both the basement and BFU are uplifted by southward verging monoclinal structures.

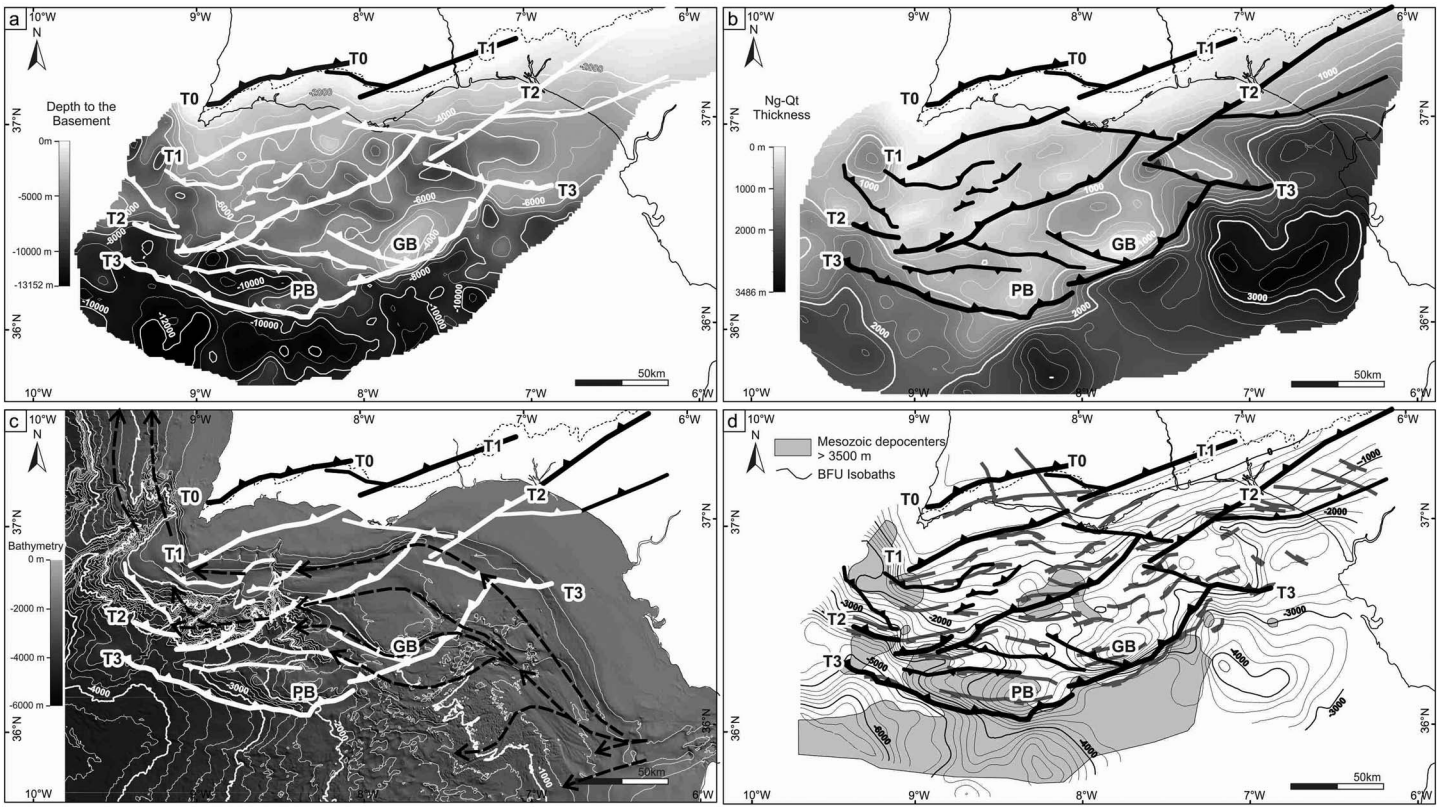


**Figure 14.** Structural maps of SW Iberian margin. (a) Depth map of the top of basement and location of the main thrust faults responsible for its uplift in Cenozoic times. (b) True vertical thickness (TVT) of the Neogene/Quaternary succession and location of basement thrusts. Note the impact of thrusts on the location of post-Oligocene depocenters. (c) Seabed bathymetry and location of basement thrusts. The black dashed arrows indicate the MOW currents taken from *Hernández-Molina et al*. [2016]. Note the control exerted locally by thrusts T2, T3, and their lateral ramps on the trajectories of the MOW currents. (d) Depth map of the BFU and basement thrust traces, with an overlay of Mesozoic age extensional faults in grey and Mesozoic depocenters greater than 3500 m thick in grey shade. See discussion in text.

The timing of the BFU relative to the basement uplift structures mentioned above makes the BFU an ideal surface to discriminate structures that have uplifted due to basement uplift in the Cenozoic. Note, for instance, that a major step in the basement seen south of the Ruivo well (Figure 11b) that is interpreted to respond to a major Mesozoic extensional fault has no major impact on the BFU geometry, whereas other major steps such as that south of the Portimão Bank (Figure 11d) does coincide with a step in the BFU, indicating a post-Mesozoic uplift.

To correlate the steps in basement at the scale of the basin, the BFU surface has been mapped in 3-D (Figure 13). This map shows a number of WSW-ENE trending steps, which, in combination with the available seismic and outcrop data, have been used to define four main steps in the regional elevation of the BFU and of the basement (Figure 14a) related to Cenozoic to recent shortening. Uplift along the Guadalquivir Bank and the onshore northern limit of the basin are interpreted to be related to underlying south verging basement-involving thrusts. These two fault structures, labeled T0 and T3 in Figures 11 and 13, bound the domain of contractional structures documented in this paper. In between these two structures two other main steps can be identified. One is the monocline in Figure 10, labeled T2. The fourth structure is T1 (Figures 11b and 11d). Toward the west T1 corresponds to the Carcavai fault zone, an ENE-WSW compressional fault [e.g., *Carvalho et al*., 2012].

The four main thrusts identified in the Algarve Basin locally deviate from their dominant WSW-ENE trend, forming a set of oblique ramps of the thrust system with NW-SE orientation (Figure 13). One of the most prominent of these is that formed onshore, where the northern thrust (T0) merges with thrust T1 (Figure 13). This oblique ramp is responsible for the jog in the map expression of the northern outcrop margin of the basin. Other oblique ramps are also visible between T2 and T3, at the western end of the Guadalquivir

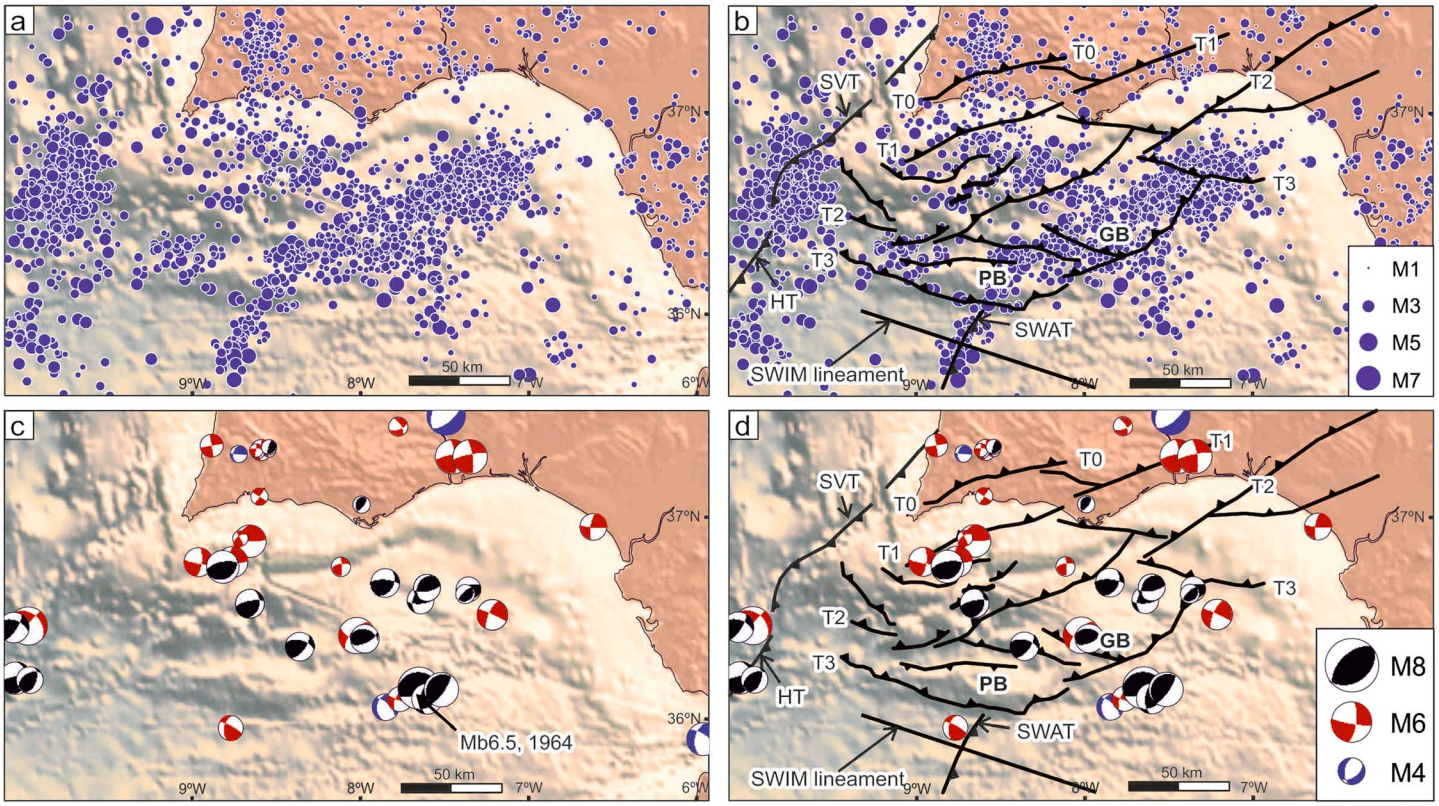


**Figure 15.** (a) Earthquake epicenters in SW Iberia, sized as a function of magnitude (modified after *Palano et al.* [2013]). The earthquakes were recorded between 1951 and 2010, with magnitudes between 2.0 and 8.0 down to ~30 km depth. (b) Location of the earthquake epicenters relative to the thrusts described in this paper. (c) Lower hemisphere, equal area projection for fault-plane solutions, complied from several earthquakes: red for strike-slip faulting, black for thrust faulting, and blue for normal faulting, modified after *Palano et al.* [2013]. (d) Location of the focal mechanisms relative to the thrust faults described in the paper. GB: Guadalquivir Bank, PB: Portimão Bank, HT: Horseshoe Thrust, SVT: São Vicente Thrust, SWAT: Southwest Algarve Thrust.

Bank (Figure 13). The western margin of the Algarve Basin is also characterized by a swing in the strike of basement thrusts to a NW-SE strike (Figure 13).

Thrust T2 runs south of the present-day southern Portuguese coastline and parallel to it east of Faro. T1 also runs roughly parallel to the coast east of Faro up to the Spanish border (in the order of 50 km) and accounts for the basement uplift that brings the outcrop margin of the basin some 20 km south in the eastern Algarve. At least in this eastern sector, it appears that both T1 and T2 probably exert a control on the present-day coastline.

In the offshore, thrusts T1, T2, and T3 also exert a control on the Neogene-Quaternary depocenters (Figure 14 b) and the present-day bathymetry and contouritic moats (Figures 7, 8, and 14c). Whereas the correlation between individual thrusts and Neogene-Quaternary depocenters or bathymetry is not one to one, it is evident that thrusts T2 and T3 exert a strong control on the thickness of Neogene-Quaternary sediments (Figure 14b) and bathymetry locally follows the trend of the main thrusts (particularly T3 and the western part of T2; Figure 14c). The oblique structures linking the main thrusts also have a marked impact on the trace of the basement outcrop (as discussed above) and in controlling some Neogene-Quaternary depocenters (for structures linking T3 and T2) and bathymetry in the central part of the basin and along its western limit.

### 5.2. Neotectonics

The system of basement-involving thrusts (T0 through T3 and oblique branches) identified in this study are observed to locally control the present-day bathymetry and contourite currents of the MOW (Figure 14c). This correlation may indicate neotectonic activity of these thrusts, but it could also result from present-day currents and seabed adapting to an inherited (pre-Quaternary) bathymetry (Figure 14). However, when overlying the map of thrusts identified in this study on maps of instrumental seismicity [*Ribeiro et al.*, 1996;

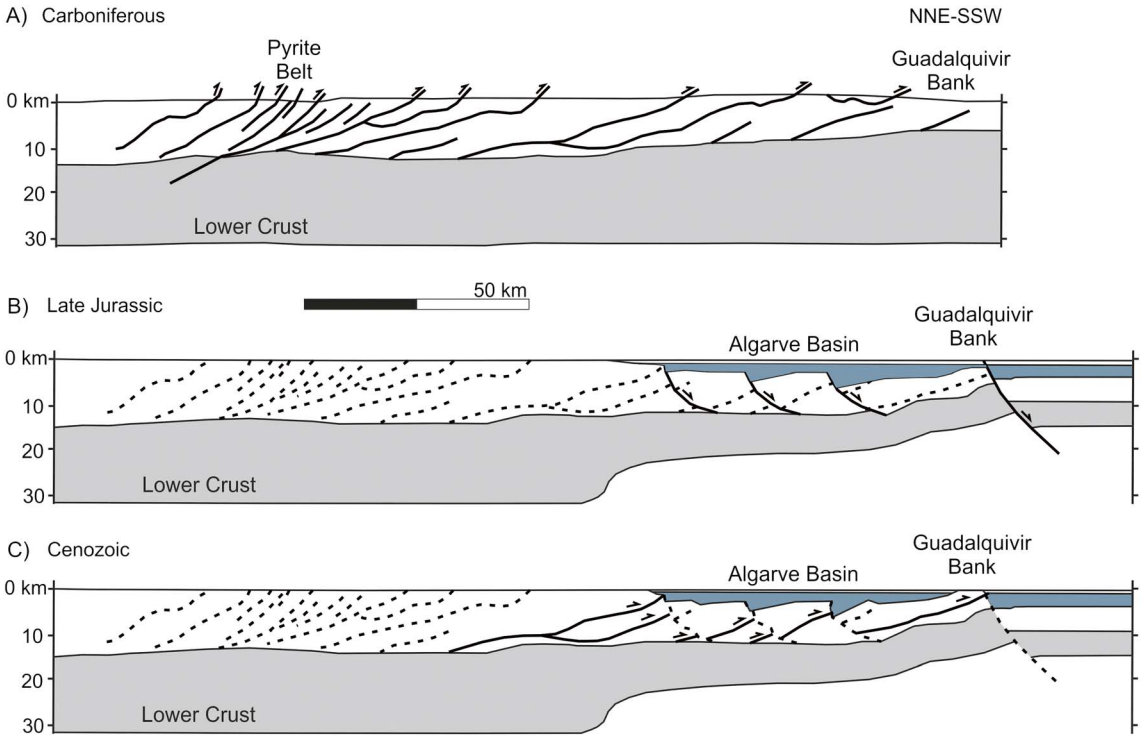


**Figure 16.** Synthetic crustal cross section of the SW Iberian Margin at key time steps. (a) At the end of Variscan thrusting (Carboniferous). (b) At the end of Jurassic extension. (c) During Cenozoic thrusting. The black lines show the faults active at each time step. The dashed black lines show the inactive faults. Modified after *Vegas et al.* [2004].

*Pedrera et al.*, 2011], it can be seen that the main cluster of seismic events in the Gulf of Cadiz sits immediately north of the Guadalquivir and Portimão Banks and associated thrust T3 (Figure 15b). This thrust is the one that has the strongest imprint on bathymetry, hence indicating that bathymetric expression of the thrusts can be related to neotectonic activity. Furthermore, thrusting on T3 is supported by the fact that focal mechanisms estimated in this area are compatible with an E-W to WSW-ENE trending thrust (Figures 15c and 15d) and the location of the epicenters is consistent with a northward dipping T3, as surface dipping to the north mapped from epicenters by *Palano et al.* [2016]. A similar relationship can be observed between minor clusters further north and the T2 thrust and for the minor oblique thrusts between T2 and T1 (Figure 15b). The fact that the other focal mechanisms derived for the Algarve Basin indicate strike slip along N-S and E-W conjugates or NW-SE and NE-SW conjugates (Figure 15d) is taken to respond to the presence of NW-SE to N-S trending tear faults and lateral ramps in the main thrust system defined by T0–T3 (Figure 13). The intermediate depth of these earthquakes [*Palano et al.*, 2013], ranging from crust to mantle, supports the idea that these events are linked to basement or crustal faults. We therefore consider that the basement thrust system described in this paper and their associated structures (tear faults and lateral ramps) are the most likely culprits for the seismic activity recorded in the Algarve Basin.

The two other evident clusters of seismic activity that can be seen in the vicinity of the Algarve Basin lie in the area of the Horseshoe, Marquês de Pombal, and São Vicente Thrusts to the west (Figures 15a and 15b) and south of the Portimão Bank and the T3 Thrust. The cluster south of the Portimão Bank runs along a NE-SW trend that cannot be correlated to any known structure (Figures 15a and 15b) but is parallel to the thrusts further west (Gorringe, Horseshoe, Marquês de Pombal, and São Vicente) and is therefore interpreted to be associated to a structure not yet identified on seismic and proposed here as the Southwest Algarve Thrust (Figure 15b). This structure has not been documented on seismic as it lies under the AWGC and poor seismic image precludes its identification.

The generalized absence of seismic activity to the south of the Algarve Basin, in the domain nowadays covered by the AUGC and AWGC (Figure 16), coincides with the area that could potentially be interpreted to be oceanic crust [*Sallarès et al.*, 2011; *Martínez-Loriente et al.*, 2014] and indicates that deformation

within the AUGC and the AWGC is reduced at present, or nonseismic and shallow and dominated by deformation related to shale and evaporite mobility [*Medialdea et al*., 2004].

### 5.3. Timing

The tectono-sedimentary relationships observed so far in the Algarve Basin are consistent with two main broad stages of basin evolution: one lasting from Triassic to Early Cretaceous dominated by extensional tectonics and one lasting from possibly Late Cretaceous, and certainly from Oligocene, to Present dominated by compressional tectonics. These two stages are in turn coherent in the framework of Mesozoic opening of the Tethys and Atlantic Oceans and the mainly Cenozoic convergence between Africa and Eurasia [*Schettino and Turco*, 2011].

As discussed above, multiple unconformities in the Miocene to Recent sediments in the Algarve Basin record the contractional deformation of the offshore structures (e.g., Figure 6) [*Hernández-Molina et al*., 2016]. The oldest Cenozoic contractional deformation is that related to the reactivation of salt walls documented in the Esperança Salt area of Paleogene age (Figure 5). A similar magnitude of Paleogene deformation has not been recognized for other structures in the area with the available data. Nonetheless, the Paleogene is observed to thin (depositionally) onto some of the offshore thrusts (for instance, onto the monocline related to T2; on the northern end of Figure 10), indicating that basement uplift might have started as early as Paleogene. Thrusting on T2 and tilting and folding north of the Esperança Salt in the Paleogene could tentatively be the source of the shortening absorbed by the salt walls on the Esperança Salt.

The Paleogene is also observed to thin or be absent over the other two basement thrusts in the offshore (as occurs above the Guadalquivir Bank in Figure 8 or above all the thrusts in Figures 11b and 11d). However, in some cases this thinning or absence of the Paleogene can be interpreted to be either depositional (recording Paleogene age uplift) or erosional (implying late Paleogene or early Miocene uplift prior to incision by the BFU). In many cases, the case for late Paleogene or early Miocene pre-BFU uplift and truncation of the Paleogene or even Cretaceous is evident (Figure 8).

For the remainder of the Neogene to Quaternary two main stages of deformation are observed in the area. For one, emplacement of the AWGC and AUGC in the area is of middle to late Miocene age. Sediments that seal movement of these units are later folded in late Pliocene times and onlapped by latest Pliocene and Quaternary sediments (consistent with the tectonic control on contourite deposits proposed by *Hernández-Molina et al*. [2016]). More recent deformation has not been documented based on seismic interpretation, but evidence of neotectonic activity discussed above indicates that one final stage of deformation is currently active.

The stages of deformation documented in the offshore Algarve Basin are consistent with those defined by other authors in the area [*Terrinha*, 1998; *Roque*, 2007] who interpret four main stages of contractional deformation: (1) Late Cretaceous to Paleogene, (2) late Oligocene, (3) middle to late Miocene, and (4) late Pliocene to Present.

### 5.4. Tectonic Inheritance and Basin Inversion of the Algarve Basin

Extension during the Mesozoic in southern Iberia led to the development of E-W to WSW-ENE trending extensional faults [*Terrinha*, 1998; *Vera*, 1998; *Martínez del Olmo*, 2002; *Ramos et al*., 2016] that controlled Triassic-Jurassic depocenters (units synchronous with the main stage of extension). This trend is strongly coincident with the strike of Cenozoic contractional structures (thrusts and monoclines of the BFU) and roughly perpendicular to present-day maximum shortening directions [*Olaiz et al*., 2009; *Pérez-Peña et al*., 2010; *Muñoz-Martín et al*., 2012]. The strike of the extensional faults, perpendicular to shortening, coupled with the fact that some faults are interpreted to have had low angle of dip prior to Cenozoic shortening (e.g., faults south of the Guadalquivir Bank; Figure 7), makes them good candidates for reactivation [*Letouzey*, 1990]. However, there appears to be no direct correlation between inversion and preexisting extensional structures (Figure 14d). Only the Portimão Bank has been documented as an inverted half-graben (Figure 10) [*Terrinha et al*., 2009]. For the rest, onshore extensional faults have been observed to accommodate buttressing but no fault reactivation [*Ramos et al*., 2016]. And in the offshore the only contractional structure that coincides with a major basin-bounding extensional fault is thrust T3, whose trace coincides with the northern limit of a major Mesozoic depocenter. However, as opposed to reactivating the fault responsible for the depocenter, thrust T3 dips in the opposite direction and causes inversion by steepening the extensional fault.

This opposing dip of Cenozoic thrusts and Mesozoic extensional faults is one of the most peculiar aspects of the inversion experienced by the Algarve Basin. Throughout the basin, thrusts are north dipping (south directed), while the extensional faults are dominantly south dipping (Figures 5, 9, 11, and 14). This style has already been documented at outcrop scale in the Algibre Thrust by *Ramos et al*. [2016]. Also, in a context equivalent to the offshore Algarve Basin, inversion in the NW Iberian passive margin shows similar contractional structures, where major extensional faults are inverted by a thrust fault with opposing dip [*Tugend et al*., 2014].

A possible origin for this anomalous inversion style in the SW Iberian margin is the impact of basement fabrics on structural development. SW Iberia was located in the foreland fold-and-thrust belt of the Variscan orogen. Basement in the area is dominated by strongly deformed Carboniferous flysch sediments affected by northward dipping, southward directed thrusts and by regional cleavage dipping to the N/NE (Figure 16a) [*Vegas*, 1980; *Soriano*, 1996; *Díaz Azpiazu et al*., 2004; *Marques et al*., 2010; *Pereira et al*., 2012]. During Mesozoic extension, initial extension (in the Triassic) probably reactivated this fabric leading to small-displacement, northward dipping normal faults with relatively shallow detachments [*Terrinha*, 1998; *Ramos et al*., 2016]. As extension progressed, southward dipping regional-scale faults became more efficient at accommodating increasing extension, leading to the regional pattern of WSW-ENE striking, southward dipping faults (Figure 1 b). Finally, basin inversion during the Cenozoic led to the reactivation of the low-angle thrusts and cleavage within the Carboniferous and deeper units (now near midcrustal depths; Figure 16c).

A similar style of inversion has been documented in the Moroccan Atlas. *Teixell et al*. [2003] and *Domènech* [2015] have documented multiple examples where thrusts steepen or crosscut preexisting extensional faults dipping in the opposite direction. The result is geometries very similar to those observed in the Algarve Basin (Figure 17a). *Teixell et al*. [2003] and *Domènech* [2015] have not proposed a cause for this style of inversion, but a similar basement and the location of the High Atlas in a context similar to the Algarve with respect to the Variscan orogen (southern foreland [*Simancas et al*., 2005]) provide support to the analogy in the deformation style.

*Carrera and Muñoz* [2013] also describe a similar example of tectonic inversion in the Cordillera Oriental of the Argentine Andes. There, the basement fabrics in the Precambrian sedimentary rocks caused the Andean contractional structures to develop differently from the Cretaceous extensional system.

### 5.5. Thick-Skinned Cenozoic Deformation in the Iberian Plate

The tectonic style of broad basement uplifts described in this paper for the Algarve Basin is not unique in the Iberian plate. The mountain ranges found in the interior of the Iberian plate (Figure 1b) are also characterized by thick-skinned contractional features.

These mountain ranges also display structures that in detail are analogous to those described in the Algarve Basin. For instance, in the eastern Guadalquivir Basin, immediately south of the eastern termination of the Sierra Morena, *Pedrera et al*. [2013] describe NE-SW trending monoclines deforming the overlying Jurassic in a manner very similar to the stair-stepped geometry seen in the Algarve Basin, also of late Miocene age (Figure 17b).

The southern border thrust of the eastern segment of the Spanish Central System is also similar to the Algarve structures. It is a blind thrust and is expressed at surface by a large NE-SW fold propagation fault (Figure 17c) [*De Vicente et al*., 2007]. The basement in the hanging wall of this thrust (of granitic composition) is cut by two north directed back thrusts (Figure 17c) [*De Vicente et al*., 2007], as occurs in the Guadalquivir Bank (Figures 7 and 8). Along the northern margin of the chain, the subhorizontal schistosity of the Variscan basement (metasediments) favors the formation of thrusts that generate a sequence of monoclines and tight anticlines with barely any fault displacement in the sedimentary cover similar to the nature of thrusts T0 to T3 (Figure 17d) [*De Vicente et al*., 2007]. The difference in tectonic styles between north and south resides in the different basement lithology [*De Vicente and Muñoz-Martín*, 2013].

### 5.6. Shortening Estimates and Correlation to Other Structures

Shortening is accommodated in the SW Iberian margin by thrusts or zones of distributed basement shearing. The uplift caused by these structures can range from 1 km (e.g., monoclines in Figure 11) to 3 km (Guadalquivir Bank in Figure 8). At the highest spot of the Guadalquivir Bank, at its western end, the uplift caused by thrusting has been estimated to be in excess of 5 km, probably related to the intersection of a

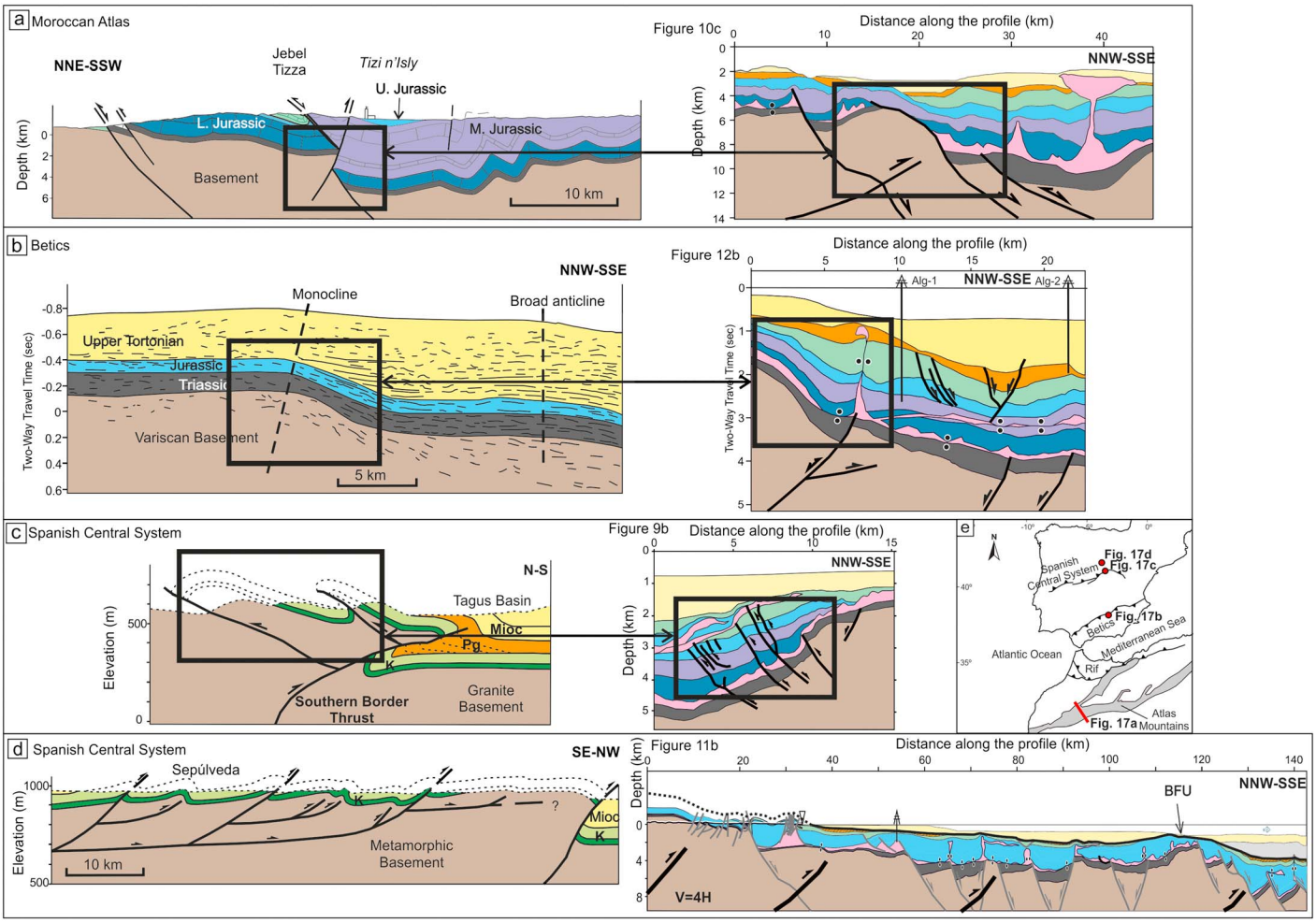


**Figure 17.** Analogue examples for the basement-involved tectonic style in SW Iberia. (a) Cross section through the high Atlas of Morocco, modified after *Teixell et al.* [2003], and the Portimão Bank (Figure 9). (b) South directed monocline in the Betics, modified after *Pedrera et al.* [2013], and the monocline above T2 (Figure 12). (c) Simplified cross section of the Tortuero back thrusting system and the back thrusts on the Guadalquivir Bank (Figure 9). (d) Sepúlveda imbricate thrust system (Mioc: Miocene, K: Cretaceous) and section across the Algarve Basin (Figure 11b). Both sections are vertically exaggerated. (Figures 17c and 17d) The examples are cross sections across the Spanish Central System, modified after *De Vicente et al.* [2007]. (e) Small inset location map for the sections presented in this figure. L., M., and U. Jurassic: Lower, Middle, and Upper Jurassic respectively; Mioc: Miocene; Pg: Paleogene.

frontal and lateral ramp of thrust T3 (Figure 13). The horizontal shortening required to generate these magnitudes of uplift is difficult to estimate and depends greatly on the estimates of depth to detachment. Restoration of some key profiles (e.g., Figure 8) and estimates of the unfolded (or untilted) length of the preinversion units allow us to estimate a horizontal shortening for the entire margin of roughly 5–10 km. This represents a shortening of less than 10% of the entire SW Iberian margin in the Algarve Basin, which is roughly 150 km wide at present day [e.g., *Terrinha*, 1998].

The amount of shortening estimated for the Algarve Basin can therefore be considered to be consistent with the approximately 20 km of NW-SE shortening estimated for the Gorringe Bank (the main contractional structure west of the Algarve Basin on the Nubia-Iberia boundary) [*Galindo-Zaldívar*, 2003; *Jiménez-Munt et al.*, 2010]. The age of deformation for the Gorringe Bank (Oligocene to Miocene; according to *Jiménez-Munt et al.* [2010]) is also broadly consistent with the earliest stages of deformation documented here for the Algarve Basin.

Estimates of basement shortening to the east along the Nubia-Iberia boundary are hindered by the presence of the allochthonous units of the Betic-Rif orogen that mask the basement structure. Furthermore, the presence of subduction processes east of the Gibraltar Arc [*Pedrera et al.*, 2011; *Vergés and Fernàndez*, 2012]

implies that the magnitude of Africa-Eurasia convergence is greater eastward and that it is absorbed by other mechanisms not seen west of the Gibraltar Arc. Nonetheless, Neogene deformation under the Guadalquivir foreland basin such as that documented by *Pedrera et al*. [2013] or the structures responsible for the uplift of the Sierra Morena [*Stapel*, 1999] are the likely continuation of the Cenozoic thrusts described in the Algarve Basin. In particular, T2 and T1 can be correlated to the east with the southern limit of the Sierra Morena (Figure 1b). The Sierra Morena is a currently tectonically active mountain chain [*Herraiz et al*., 1996; *Stich et al*., 2006] and has also recorded significant uplift during the Neogene [*Stapel*, 1999]. Its southern margin is defined by a very sharp lineament (easily seen on satellite imagery and topography) that runs from the northern coast of the Gulf of Cadiz for over 200 km to the ENE (Figure 1b). This orientation crosscuts the Variscan structural trend (WNW-ESE in the Sierra Morena) and is perpendicular to the present-day maximum horizontal stress [*Cloetingh and Burov*, 1996], which supports the interpretation of the Sierra Morena range as an upper crust antiform associated to the presence of a south directed crustal-scale blind thrust [*De Vicente et al*., 2007].

### 5.7. Alternative Interpretations for Basement Deformation

Two alternatives have been contemplated for interpreting the source of basement deformation in the Algarve Basin. One is the possible origin of some of the basement structures (in particular the Guadalquivir Bank) as a westward propagating Subduction-Transform Edge Propagator (STEP) fault [*Govers and Wortel*, 2005]. The presence of a STEP fault along the northern limit of the Alborán block in an early stage of its evolution was proposed by *van Hinsbergen et al*. [2014]. Whereas the Guadalquivir Bank is indeed in a position that could be consistent for a STEP fault ahead of the propagating Gibraltar Arc subduction zone, such an interpretation would not account for the origin of the other basement structures observed in the basin. Furthermore, STEP faults are expected to lead dominantly to subsidence, not uplift as is observed in the Guadalquivir Bank. Neither could a STEP fault account for uplift as early as Oligocene (when the Gibraltar subduction zone was much further east [*Vergés and Fernàndez*, 2012]) nor is it compatible with the lack of evidence of slab tear along strike of the Guadalquivir Bank under the Betics [*Vergés and Fernàndez*, 2012].

The second alternative interpretation for basement deformation is strike-slip dominated deformation, in line with observations of strike-slip features in the area [*Zitellini et al*., 2009; *Carvalho et al*., 2012]. Once again, this possibility would be at odds with the dominant deformation mechanism observed for Cenozoic deformation in the Iberian plate. Furthermore, the main structures generating basement uplift in the Algarve Basin are mostly perpendicular to the maximum horizontal stress [*Olaiz et al*., 2009; *Muñoz-Martín et al*., 2012] and the recent convergence between Africa and Eurasia [*Rosenbaum et al*., 2002], making contractional structures the most likely elements driving deformation in the area. Extensional faulting of Cenozoic age in this area is limited to areas of mobile substrate (shale or evaporites [e.g., *Medialdea et al*., 2004; *Matias et al*., 2011]) and is therefore inferred to be related to shallow causes and not basement deformation.

### 5.8. Implications for Initial Stages of Passive Margin Inversion

Just as the inheritance of basement fabric appears to have had a strong control on inversion, crustal-scale structure may also have played a role in the localization of inversion structures. Some of the locations of major basement uplift documented in this margin coincide with the extensional faults with the largest throws (for instance T3 in Figure 11b or T2 in Figure 11d). Crustal-scale control on inversion is also observed in the western and northern Iberian margin. In the western Iberian margin *Peron-Pinvidic et al*. [2008] interpret that inversion locates only above continental mantle exhumed during extension. In northern Iberia, *Tugend et al*. [2014] suggest that inversion concentrates on thrusts that crosscut basinward dipping, crustal-scale faults in the domains of greatest extension of the margin. However, in both cases, inversion occurs in the most distal domain, similar to that documented by *Mohn et al*. [2012]. In the case of SW Iberia, however, crustal heterogeneities could be responsible for inversion across the necking domain of the rifted margin.

Finally, shortening is also observed in the shallowest units of the Algarve Basin. Contraction within the Mesozoic stratigraphy is driven by shortening at crustal scale, but its tectonic style and the wavelength of its structures are controlled by the Triassic evaporites acting as a detachment.

The result is a system in which deformation is partitioned and localized by the presence of heterogeneities within the rifted structure of the margin, the prerift basement, and the synrift stratigraphy.

## 6. Conclusions

The convergence of Africa and Eurasia during the Cenozoic has led to the formation of a system of roughly E-W to NE-SW regional-scale thrusts that extend from the Gorringe Bank in the west to the Betic orogen in the east (the Guadalquivir Basin and Sierra Morena). Four main, south verging thrusts, spaced at 20–50 km, have been identified in this system. Each thrust is associated to a southward dipping monocline, and they are interpreted to be deeply rooted in the basement and reactivate inherited Paleozoic northward dipping fabric (cleavage and thrusts). Extensional faults related to Mesozoic rifting are in most cases folded and steepened by these thick-skinned thrusts, leading to an inverted margin in which extensional faults have not been reactivated. Deformation in Mesozoic and Cenozoic strata is accommodated by buttressing, minor thrusting, and reactivation of diapirs.

At least four main stages of shortening have been documented for the thrusts and associated structures inverting the SW Iberian margin: Late Cretaceous to early Paleogene, late Paleogene to early Miocene, middle to late Miocene, and late Pliocene to present day. The present-day kinematics of these thrusts is compatible with the main compressive direction calculated from earthquake mechanisms and from GPS plate kinematics. These thrusts are considered to be responsible for the present-day seismic activity observed in SW Iberia.

**Acknowledgments**

This study was funded by Repsol Exploración (Madrid) and partially financially supported by the SALTECRES project (CGL2014-54118-C2-1-R MINECO/FEDER, UE). Adrià Ramos thanks Repsol Exploración for his Ph.D grant. The authors wish to thank Álvaro Arnaiz and Repsol Portugal Exploration Team for their support and enthusiasm. The authors also wish to thank S. Martínez-Loriente, M.A. Gutscher, and a third anonymous reviewer for their in-depth reviews and discussion that have greatly helped us to improve this paper. We also acknowledge Schlumberger and Midland Valley for the academic software licenses used for seismic interpretation and cross-section construction, respectively. Repsol and Partex-Oil&Gas provided us their proprietary vintage seismic surveys and a 3-D seismic cube, published with their permission. Seismic lines of the PDT00-PD00 survey have been provided by TGS and published with the permission of TGS (http://www.tgs.com). The seismic PDT00-PD00 survey is available for purchase from TGS and Entidade Nacional para o Mercado de Combustibles (http://www.enmc.pt).

## References

Arsenikos, S., D. Frizon de Lamotte, N. Chamot-Rooke, G. Mohn, M.-C. Bonneau, and C. Blanpied (2013), Mechanism and timing of tectonic inversion in Cyrenaica (Libya): Integration in the geodynamics of the East Mediterranean, *Tectonophysics*, *608*, 319–329, doi:10.1016/j.tecto.2013.09.025.

Boldreel, L. O., and M. S. Andersen (1993), Late Paleocene to Miocene compression in the Faeroe-Rockall area, *Geol. Soc. London, Pet. Geol. Conf. Ser.*, *4*, 1025–1034, doi:10.1144/0041025.

Brune, S., C. Heine, P. D. Clift, and M. Pérez-Gussinyé (2016), Rifted margin architecture and crustal rheology: Reviewing Iberia-Newfoundland, central South Atlantic, and South China Sea, *Mar. Pet. Geol.*, doi:10.1016/j.marpetgeo.2016.10.018.

Carrera, N., and J. A. Muñoz (2013), Thick-skinned tectonic style resulting from the inversion of previous structures in the southern Cordillera Oriental (NW Argentine Andes), *Geol. Soc. London, Spec. Publ.*, *377*(1), 77–100, doi:10.1144/SP377.2.

Carrilho, F., P. Teves-Costa, I. Morais, J. Pagarete, and R. Dias (2004), GEOALGAR project: First results on seismicity and fault-plane solutions, *Pure Appl. Geophys.*, *161*(3), 589–606, doi:10.1007/s00024-003-02464-3.

Carvalho, J., H. Matias, T. Rabeh, P. T. L. Menezes, V. C. F. Barbosa, R. Dias, and F. Carrilho (2012), Connecting onshore structures in the Algarve with the southern Portuguese continental margin: The Carcavai fault zone, *Tectonophysics*, *570–571*, 151–162, doi:10.1016/j.tecto.2012.08.011.

Cloetingh, S., and E. B. Burov (1996), Thermomechanical structure of European continental lithosphere: Constraints from rheological profiles and EET estimates, *Geophys. J. Int.*, *124*(3), 695–723, doi:10.1111/j.1365-246X.1996.tb05633.x.

Cobbold, P. R., K. E. Meisling, and V. S. Mount (2001), Reactivation of an obliquely rifted margin, Campos and Santos Basins, southeastern Brazil, *AAPG Bull.*, *85*(11), 1925–1944.

Custódio, S., N. A. Dias, F. Carrilho, E. Góngora, I. Rio, C. Marreiros, I. Morais, P. Alves, and L. Matias (2015), Earthquakes in western Iberia: Improving the understanding of lithospheric deformation in a slowly deforming region, *Geophys. J. Int.*, *203*(1), 127–145, doi:10.1093/gji/ggv285.

Custódio, S., G. Silveira, L. Matias, I. Mata, C. Matos, J. M. Palma-Oliveira, F. Rocha, and F. C. Lopes (2016), Educating for earthquake science and risk in a tectonically slowly deforming region, *Seismol. Res. Lett.*, *87*(3), 773–782, doi:10.1785/0220150239.

De Vicente, G., and A. Muñoz-Martín (2013), The Madrid Basin and the Central System: A tectonostratigraphic analysis from 2D seismic lines, *Tectonophysics*, *602*, 259–285, doi:10.1016/j.tecto.2012.04.003.

De Vicente, G., and R. Vegas (2009), Large-scale distributed deformation controlled topography along the western Africa–Eurasia limit: Tectonic constraints, *Tectonophysics*, *474*(1–2), 124–143, doi:10.1016/j.tecto.2008.11.026.

De Vicente, G., et al. (2004), Evolución geodinámica y cenozoica de la placa ibérica y su registro en el antepaís, in *Geología de España*, edited by J. A. Vera, pp. 597–602, SGE-IGME, Madrid.

De Vicente, G., R. Vegas, A. Muñoz-Martín, P. Silva, P. Andriessen, S. Cloetingh, J. Gonzalezcasado, J. Vanwees, J. Alvarez, and A. Carbo (2007), Cenozoic thick-skinned deformation and topography evolution of the Spanish Central System, *Global Planet. Change*, *58*(1–4), 335–381, doi:10.1016/j.gloplacha.2006.11.042.

DeMets, C., R. G. Gordon, and D. F. Argus (2010), Geologically current plate motions, *Geophys. J. Int.*, *181*(1), 1–80, doi:10.1111/j.1365-246X.2009.04491.x.

Dercourt, J., et al. (1986), Geological evolution of the Tethys belt from the Atlantic to the Pamirs since the LIAS, *Tectonophysics*, *123*(1–4), 241–315, doi:10.1016/0040-1951(86)90199-X.

Dewey, J. F., W. C. Pitman, W. B. Ryan, and J. Bonnin (1973), Plate tectonics and the evolution of the Alpine system, *Geol. Soc. Am. Bull.*, *84*(10), 3137–3180.

Dewey, J. F., M. L. Helman, S. D. Knott, E. Turco, and D. H. W. Hutton (1989), Kinematics of the western Mediterranean, *Geol. Soc. London, Spec. Publ.*, *45*(1), 265–283, doi:10.1144/GSL.SP.1989.045.01.15.

Dias, R., and J. Cabral (1997), Neotectonic crustal vertical movements in Algarve (southern Portugal) 3a Conf. Anu. Grupo Geol. Estrutural E Tectónica Soc Geol Port. Livro Resumos.

Díaz Azpiazu, M., A. Castro, C. Fernández, S. López, J. C. Fernández Caliani, and I. Moreno-Ventas (2004), The contact between the Ossa Morena and the South Portuguese zones: Characteristics and significance of the Aracena metamorphic belt, in its central sector between Aroche and Aracena (Huelva), *J. Iber. Geol.*, *30*, 23–52.

Domènech, M. (2015), Rift opening and inversion in the Marrakech High Atlas: Integrated structural and thermochronologic study, PhD thesis, 157 pp., Universitat Autònoma de Barcelona.

Doré, A. G., E. R. Lundin, N. J. Kusznir, and C. Pascal (2008), Potential mechanisms for the genesis of Cenozoic domal structures on the NE Atlantic margin: Pros, cons and some new ideas, *Geol. Soc. London, Spec. Publ.*, *306*(1), 1–26, doi:10.1144/SP306.1.
Druet, M. (2016), Geodinámica del margen continental de Galicia: Estructura profunda y morfotectónica, PhD thesis, 251 pp., Universidad Complutense de Madrid, Madrid.
Duarte, J. C. (2011), Tectonics of the Gulf of Cadiz: The role of the Gibraltar Arc in the reactivation of the SW Iberia Margin, PhD thesis, 304 pp., Universidade de Lisboa.
Duarte, J. C., V. Valadares, P. Terrinha, F. Rosas, N. Zitellini, and E. Gràcia (2009), Anatomy and tectonic significance of WNW-ESE and NE-SW lineaments at a transpressive plate boundary (Nubia-Iberia), *Trab. Geol.*, *29*(29), 237–241.
Duarte, J. C., P. Terrinha, F. M. Rosas, V. Valadares, L. M. Pinheiro, L. Matias, V. Magalhães, and C. Roque (2010), Crescent-shaped morphotectonic features in the Gulf of Cadiz (offshore SW Iberia), *Mar. Geol.*, *271*(3–4), 236–249, doi:10.1016/j.margeo.2010.02.017.
Duarte, J. C., F. M. Rosas, P. Terrinha, W. P. Schellart, D. Boutelier, M.-A. Gutscher, and A. Ribeiro (2013), Are subduction zones invading the Atlantic? Evidence from the southwest Iberia margin, *Geology*, *41*(8), 839–842, doi:10.1130/G34100.1.
Faleide, J. I., F. Tsikalas, A. J. Breivik, R. Mjelde, O. Ritzmann, O. Engen, J. Wilson, and O. Eldholm (2008), Structure and evolution of the continental margin off Norway and the Barents Sea, *Episodes*, *31*(1), 82–91.
Feio, M. (1951), *A Evolução do Relevo do Baixo Alentejo a Algarve*, pp. 303–477, *Corn Serv Geol Port., t.XXXII, 2a parte*, Lisboa.
Fernández-Lozano, J. (2012), Cenozoic deformation of Iberia: A model for intraplate mountain building and basin development based on analogue modelling, PhD thesis, 173 pp., Utretcht Univ.
Flinch, J. F., and P. R. Vail (1998), Plio-Pleistocene sequence stratigraphy and tectonics of the Gibralter Arc, in *Mesozoic and Cenozoic Sequence Stratigraphy of European Basins*, vol. 60, edited by P. C. de Graciansky et al., pp. 199–208, SEPM Spec. Publ, Tulsa, Okla.
Galindo-Zaldívar, J. (2003), Active faulting in the internal zones of the central Betic Cordilleras (SE, Spain), *J. Geodyn.*, *36*(1–2), 239–250, doi:10.1016/S0264-3707(03)00049-8.
Gardosh, M. A., and Y. Druckman (2006), Seismic stratigraphy, structure and tectonic evolution of the Levantine Basin, offshore Israel, *Geol. Soc. London, Spec. Publ.*, *260*, 201–227, doi:10.1144/GSL.SP.2006.260.01.09.
Gomez, F., W. Beauchamp, and M. Barazangi (2000), Role of the Atlas Mountains (northwest Africa) within the African-Eurasian plate-boundary zone, *Geology*, *28*(9), 775–778, doi:10.1130/0091-7613(2000)28<775:ROTAMN>2.0.CO;2.
Govers, R., and M. J. R. Wortel (2005), Lithosphere tearing at STEP faults: Response to edges of subduction zones, *Earth Planet. Sci. Lett.*, *236*(1–2), 505–523, doi:10.1016/j.epsl.2005.03.022.
Gràcia, E., et al. (2003a), Mapping active faults offshore Portugal (36°N–38°N): Implications for seismic hazard assessment along the southwest Iberian margin, *Geology*, *31*(1), 83–86.
Gràcia, E., J. Dañobeitia, J. Vergés, R. Bartolomé, and D. Córdoba (2003b), Crustal architecture and tectonic evolution of the Gulf of Cadiz (SW Iberian margin) at the convergence of the Eurasian and African plates, *Tectonics*, *22*(4), 1033, doi:10.1029/2001TC901045.
Gutscher, M.-A., J. Malod, J.-P. Rehault, I. Contrucci, F. Klingelhoefer, L. Mendes-Victor, and W. Spakman (2002), Evidence for active subduction beneath Gibraltar, *Geology*, *30*(12), 1071, doi:10.1130/0091-7613(2002)030<1071:EFASBG>2.0.CO;2.
Gutscher, M.-A., S. Dominguez, G. K. Westbrook, and P. Leroy (2009), Deep structure, recent deformation and analog modeling of the Gulf of Cadiz accretionary wedge: Implications for the 1755 Lisbon earthquake, *Tectonophysics*, *475*(1), 85–97, doi:10.1016/j.tecto.2008.11.031.
Handy, M. R., S. M. Schmid, R. Bousquet, E. Kissling, and D. Bernoulli (2010), Reconciling plate-tectonic reconstructions of Alpine Tethys with the geological–geophysical record of spreading and subduction in the Alps, *Earth-Sci. Rev.*, *102*(3–4), 121–158, doi:10.1016/j.earscirev.2010.06.002.
Hernández-Molina, F. J., et al. (2014), Onset of Mediterranean outflow into the North Atlantic, *Science*, *344*(6189), 1244–1250, doi:10.1126/science.1251306.
Hernández-Molina, F. J., et al. (2016), Evolution of the gulf of Cadiz margin and southwest Portugal contourite depositional system: Tectonic, sedimentary and paleoceanographic implications from IODP expedition 339, *Mar. Geol.*, *377*, 7–39, doi:10.1016/j.margeo.2015.09.013.
Herraiz, M., G. de Vicente, R. Lindo, and J. G. Sánchez-Caba~nero (1996), Seismotectonics of the Sierra Albarrana area (southern Spain). Constraints for a regional model of the Sierra Morena-Guadalquivir Basin limit, *Tectonophysics*, *266*(1–4), 425–442, doi:10.1016/S0040-1951(96)00201-6.
Hill, K. A., G. T. Cooper, M. J. Richardson, C. J. Lavin, K. A. Hill, G. T. Cooper, M. J. Richardson, and C. J. Lavin (1994), Structural framework of the eastern Otway Basin: Inversion and interaction between two major structural provinces, structural framework of the eastern Otway Basin, *Explor. Geophys. Explor. Geophys.*, *25*(2), 79–87, doi:10.1071/EG994079.
Indrevær, K., R. H. Gabrielsen, and J. I. Faleide (2016), Early Cretaceous synrift uplift and tectonic inversion in the Loppa High area, southwestern Barents Sea, Norwegian shelf, *J. Geol. Soc.*, doi:10.1144/jgs2016-066.
IOC, IHO, and BODC (2003), *Centenary Edition of the GEBCO Digital Atlas, published on CDROM on behalf of the Intergovernmental Oceanographic Commission and the International Hydrographic Organization as part of the General Bathymetric Chart of the Oceans*, British Oceanographic Data Centre, Liverpool, U. K.
Iribarren, L., J. Vergés, F. Camurri, J. Fullea, and M. Fernàndez (2007), The structure of the Atlantic–Mediterranean transition zone from the Alboran Sea to the Horseshoe Abyssal Plain (Iberia–Africa plate boundary), *Mar. Geol.*, *243*(1–4), 97–119, doi:10.1016/j.margeo.2007.05.011.
Jiménez-Munt, I., M. Fernàndez, J. Vergés, J. C. Afonso, D. Garcia-Castellanos, and J. Fullea (2010), Lithospheric structure of the Gorringe Bank: Insights into its origin and tectonic evolution, *Tectonics*, *29*, TC5019, doi:10.1029/2009TC002458.
Johnson, H., J. D. Ritchie, K. Hitchen, D. B. Mcinroy, and G. S. Kimbell (2005), Aspects of the Cenozoic deformational history of the Northeast Faroe-Shetland Basin, Wyville-Thomson Ridge and Hatton Bank areas, *Geol. Soc. London, Pet. Geol. Conf. Ser.*, *6*, 993–1007, doi:10.1144/0060993.
Lundin, E., and A. G. Doré (2002), Mid-Cenozoic post-breakup deformation in the "passive" margins bordering the Norwegian-Greenland Sea, *Mar. Pet. Geol.*, *19*, 79–93, doi:10.1016/S0264-8172(01)00046-0.
Lanaja, J. M. (1987), *Contribución de la exploración petrolífera al conocimiento de la geología de España*, IGME, Madrid.
Ledesma, S. M. (2000), Astrobiocronología y estratigrafía de alta resolución del Neógeno de la Cuenca del Guadalquivir-Golfo de Cádiz, PhD thesis, 464 pp., Universidad de Salamanca.
Letouzey, J. (1990), Fault reactivation, inversion and fold-thrust belt, in *Petroleum and Tectonics in Mobile Belts*, edited by J. Letouzey, pp. 101–128, Technic, Paris.
Llave, E., H. Matias, F. J. Hernández-Molina, G. Ercilla, D. A. V. Stow, and T. Medialdea (2011), Pliocene–Quaternary contourites along the northern Gulf of Cadiz margin: Sedimentary stacking pattern and regional distribution, *Geo-Mar. Lett.*, *31*(5–6), 377–390, doi:10.1007/s00367-011-0241-3.

Lonergan, L., and N. White (1997), Origin of the Betic-Rif mountain belt, *Tectonics*, *16*(3), 504–522, doi:10.1029/96TC03937.
Maldonado, A., L. Somoza, and L. Pallarés (1999), The Betic orogen and the Iberian–African boundary in the Gulf of Cadiz: Geological evolution (central North Atlantic), *Mar. Geol.*, *155*(1–2), 9–43, doi:10.1016/S0025-3227(98)00139-X.
Malod, J. A., and D. Mougenot (1979), L'histoire geologique neogene du golfe de Cadix, *Bull. Soc. Geol. Fr.*, *S7–XXI*(5), 603–611, doi:10.2113/gssgfbull.S7-XXI.5.603.
Manuppella, G. (1992), *Carta geológica da região do Algarve*, Noticia explicativa da Carta Geologica da regiao do Algarve Serviços geológicos de Portugal.
Marques, F. O., J.-P. Burg, S. M. Lechmann, and S. M. Schmalholz (2010), Fluid-assisted particulate flow of turbidites at very low temperature: A key to tight folding in a submarine Variscan foreland basin of SW Europe, *Tectonics*, *29*, TC2005, doi:10.1029/2008TC002439.
Martínez del Olmo, W. (2002), Secuencias de depósito y estructuración diapírica en el Mesozoico y Neógeno del Prebético y Golfo de Valencia desde sondeos y líneas sísmicas, PhD thesis, 563 pp., Universidad Complutense de Madrid.
Martínez-Loriente, S., et al. (2013), Active deformation in old oceanic lithosphere and significance for earthquake hazard: Seismic imaging of the Coral Patch Ridge area and neighboring abyssal plains (SW Iberian Margin): Active Deformation Coral Patch Ridge, *Geochem. Geophys. Geosyst.*, *14*, 2206–2231, doi:10.1002/ggge.20173.
Martínez-Loriente, S., V. Sallarès, E. Gràcia, R. Bartolome, J. J. Dañobeitia, and N. Zitellini (2014), Seismic and gravity constraints on the nature of the basement in the Africa-Eurasia plate boundary: New insights for the geodynamic evolution of the SW Iberian margin: Thin oceanic crust at the CPR and SH, *J. Geophys. Res. Solid Earth*, *119*, 127–149, doi:10.1002/2013JB010476.
Martínez-Loriente, S., E. Grácia, R. Bartolome, H. Perea, D. Klaeschen, J. J. Dañobeitia, N. Zitellini, R. B. Wynn, and D. G. Masson (2016), Morphostructure, tectono-sedimentary evolution and seismic potential of the Horseshoe Fault, SW Iberian Margin, *Basin Res.*, doi:10.1111/bre.12225.
Martins, L. T., J. Madeira, N. Youbi, J. Munhá, J. Mata, and R. Kerrich (2008), Rift-related magmatism of the central Atlantic magmatic province in Algarve, southern Portugal, *Lithos*, *101*(1–2), 102–124, doi:10.1016/j.lithos.2007.07.010.
Matias, H. (2007), Hydrocarbon potential of the offshore Algarve Basin, PhD thesis, 324 pp., Faculdade de Ciências da Universidade Nova de Lisboa.
Matias, H., P. Kress, P. Terrinha, W. Mohriak, P. T. L. Menezes, L. Matias, F. Santos, and F. Sandnes (2011), Salt tectonics in the western Gulf of Cadiz, southwest Iberia, *AAPG Bull.*, *95*(10), 1667–1698, doi:10.1306/01271110032.
Medialdea, T., R. Vegas, L. Somoza, J. T. Vázquez, A. Maldonado, V. Díaz-del-Río, A. Maestro, D. Córdoba, and M. C. Fernández-Puga (2004), Structure and evolution of the "Olistostrome" complex of the Gibraltar Arc in the Gulf of Cádiz (eastern central Atlantic): Evidence from two long seismic cross sections, *Mar. Geol.*, *209*(1–4), 173–198, doi:10.1016/j.margeo.2004.05.029.
Michard, D., O. Frizon de Lamotte, O. Saddiqi, and A. Chalouan (2008), An Outline of the Geology of Morocco, in *Continental Evolution: The Geology of Morocco: Structure, Stratigraphy, and Tectonics of the Africa-Atlantic-Mediterranean Triple Junction*, edited by A. Michard, A. Chalouan, and O. Saddiqi, pp. 1–31, Lecture Notes in Earth Sciences, 116, Springer.
Medialdea, T., L. Somoza, L. M. Pinheiro, M. C. Fernández-Puga, J. T. Vázquez, R. León, M. K. Ivanov, V. Magalhaes, V. Díaz-del-Río, and R. Vegas (2009), Tectonics and mud volcano development in the Gulf of Cádiz, *Mar. Geol.*, *261*(1–4), 48–63, doi:10.1016/j.margeo.2008.10.007.
Mohn, G., G. Manatschal, M. Beltrando, E. Masini, and N. Kusznir (2012), Necking of continental crust in magma-poor rifted margins: Evidence from the fossil Alpine Tethys margins, *Tectonics*, *31*, TC1012, doi:10.1029/2011TC002961.
Mougenot, D. (1989), Geologia da margem portuguesa, PhD thesis, 259 pp., Univer. Pierre et Marie Curie, Paris VI.
Muñoz-Martín, A., et al. (2012), Mapa de esfuerzos activos en línea de la Península Ibérica a partir de Mecanismos Focales calculados desde el Tensor de Momento Sísmico, *Geotemas*, *13*, 1–4.
Olaiz, A. J., A. Muñoz-Martín, G. De Vicente, R. Vegas, and S. Cloetingh (2009), European continuous active tectonic strain–stress map, *Tectonophysics*, *474*(1–2), 33–40, doi:10.1016/j.tecto.2008.06.023.
Palano, M., P. J. González, and J. Fernández (2013), Strain and stress fields along the Gibraltar Orogenic Arc: Constraints on active geodynamics, *Gondwana Res.*, *23*(3), 1071–1088, doi:10.1016/j.gr.2012.05.021.
Palano, M., P. J. González, and J. Fernández (2016), Crustal deformation evidences for viscous coupling and fragmented lithosphere at the Nubia-Iberia plate boundary (Western Mediterranean), EGU General Assembly 2016, p. 12132, Vienna, Austria, 17–22 April.
Pedrera, A., et al. (2011), Is there an active subduction beneath the Gibraltar orogenic arc? Constraints from Pliocene to present-day stress field, *J. Geodyn.*, *52*(2), 83–96, doi:10.1016/j.jog.2010.12.003.
Pedrera, A., A. Ruiz-Constán, C. Marín-Lechado, J. Galindo-Zaldívar, A. González, and J. A. Peláez (2013), Seismic transpressive basement faults and monocline development in a foreland basin (eastern Guadalquivir, SE Spain), *Tectonics*, *32*(6), 1571–1586, doi:10.1002/2013TC003397.
Perconig, E. (1962), Sur la constitution géologique de l'Andalousie occidentale en particulier du bassin du Guadalquivir (Espagne méridionale), *Livre Mémoire du Professeur Paul Fallot*, *Mem. Hors-Ser. Soc. Geol. Fr.*, *1*, 229–256.
Pereira, M. F., M. Chichorro, J. B. Silva, B. Ordóñez-Casado, J. K. W. Lee, and I. S. Williams (2012), Early carboniferous wrenching, exhumation of high-grade metamorphic rocks and basin instability in SW Iberia: Constraints derived from structural geology and U–Pb and $^{40}Ar$–$^{39}Ar$ geochronology, *Tectonophysics*, *558–559*, 28–44, doi:10.1016/j.tecto.2012.06.020.
Pérez-Peña, A., J. Martín-Davila, J. Gárate, M. Berrocoso, and E. Buforn (2010), Velocity field and tectonic strain in southern Spain and surrounding areas derived from GPS episodic measurements, *J. Geodyn.*, *49*(3–4), 232–240, doi:10.1016/j.jog.2010.01.015.
Peron-Pinvidic, G., and G. Manatschal (2009), The final rifting evolution at deep magma-poor passive margins from Iberia-Newfoundland: A new point of view, *Int. J. Earth Sci.*, *98*(7), 1581–1597, doi:10.1007/s00531-008-0337-9.
Peron-Pinvidic, G., G. Manatschal, S. M. Dean, and T. A. Minshull (2008), Compressional structures on the West Iberia rifted margin: Controls on their distribution, *Geol. Soc. London, Spec. Publ.*, *306*(1), 169–183, doi:10.1144/SP306.8.
Ramos, A., L. Cascone, A. Olaiz, O. Fernández, A. Sánchez de la Muela, W. Hermoza, A. Arnaiz, and R. Rocca (2015), Crustal structure of the southern Portuguese Margin—Constraints from potential field methods, paper presented at 77th EAGE Conference and Exhibition 2015.
Ramos, A., O. Fernández, P. Terrinha, and J. A. Muñoz (2016), Extension and inversion structures in the Tethys–Atlantic linkage zone, Algarve Basin, Portugal, *Int. J. Earth Sci.*, *105*(5), 1663–1679, doi:10.1007/s00531-015-1280-1.
Ribeiro, A., M. T. Antunes, M. P. Ferreira, R. B. Rocha, A. F. Soares, G. Zbyszewski, F. M. de Almeida, D. de Carvalho, and J. H. Monteiro (1979), Introduction á la géologie générale du Portugal, 114 pp., Serviços Geológicos de Portugal, Lisboa.
Ribeiro, A., J. Cabral, R. Baptista, and L. Matias (1996), Stress pattern in Portugal mainland and the adjacent Atlantic region, West Iberia, *Tectonics*, *15*(3), 641–659, doi:10.1029/95TC03683.
Roca, E., J. A. Muñoz, O. Ferrer, and N. Ellouz (2011), The role of the Bay of Biscay Mesozoic extensional structure in the configuration of the Pyrenean orogen: Constraints from the MARCONI deep seismic reflection survey, *Tectonics*, *30*, TC2001, doi:10.1029/2010TC002735.
Roest, W. R., and S. P. Srivastava (1991), Kinematics of the plate boundaries between Eurasia, Iberia, and Africa in the North Atlantic from the Late Cretaceous to the present, *Geology*, *19*(6), 613, doi:10.1130/0091-7613(1991)019<0613:KOTPBB>2.3.CO;2.

Roque, C. (2007), Tectonostratigrafia do cenozóico das margens continentais sul e sudoeaste portuguesas: um modelo de correlação sismostratigráfica, PhD thesis, 310 pp., Universidade de Lisboa.
Rosenbaum, G., G. S. Lister, and C. Duboz (2002), Relative motions of Africa, Iberia and Europe during Alpine orogeny, *Tectonophysics*, *359*(1), 117–129.
Sallarès, V., A. Gailler, M.-A. Gutscher, D. Graindorge, R. Bartolomé, E. Gràcia, J. Díaz, J. J. Dañobeitia, and N. Zitellini (2011), Seismic evidence for the presence of Jurassic oceanic crust in the central Gulf of Cadiz (SW Iberian margin), *Earth Planet. Sci. Lett.*, *311*(1–2), 112–123, doi:10.1016/j.epsl.2011.09.003.
Sallarès, V., S. Martínez-Loriente, M. Prada, E. Grácia, C. Ranero, M.–A. Gutscher, R. Bartolome, A. Gailler, J. J. Dañobeitia, and N. Zitellini (2013), Seismic evidence of exhumed mantle rock basement at the Gorringe Bank and the adjacent Horseshoe and Tagus abyssal plains (SW Iberia), *Earth Planet. Sci. Lett.*, *365*, 120–131, doi:10.1016/j.epsl.2013.01.021.
Sartori, R., L. Torelli, N. Zitellini, D. Peis, and E. Lodolo (1994), Eastern segment of the Azores-Gibraltar line (central-eastern Atlantic): An oceanic plate boundary with diffuse compressional deformation, *Geology*, *22*(6), 555–558.
Schettino, A., and E. Turco (2011), Tectonic history of the western Tethys since the Late Triassic, *Geol. Soc. Am. Bull.*, *123*(1–2), 89–105.
Şengör, A. M. C. (1984), The Cimmeride orogenic system and the tectonics of Eurasia, *Geol. Soc. Am. Spec. Pap.*, *195*, 1–74, doi:10.1130/SPE195-p1.
Simancas, J. F., A. Tahiri, A. Azor, F. G. Lodeiro, D. J. Martínez Poyatos, and H. El Hadi (2005), The tectonic frame of the Variscan–Alleghanian orogen in southern Europe and northern Africa, *Tectonophysics*, *398*(3–4), 181–198, doi:10.1016/j.tecto.2005.02.006.
Soriano, C. (1996), Tectónica de cabalgamientos en la Faja Pirítica Ibérica (Zona Sur Portuguesa): el Antiforme de la Puebla de Guzmán, y la lámina de cabalgamiento de Sanlúcar de Guadiana, *Geogaceta*, *20*, 786–788.
Srivastava, S. P., H. Schouten, W. R. Roest, K. D. Klitgord, L. C. Kovacs, J. Verhoef, and R. Macnab (1990a), Iberian plate kinematics: A jumping plate boundary between Eurasia and Africa, *Nature*, *344*(6268), 756–759, doi:10.1038/344756a0.
Srivastava, S. P., W. R. Roest, L. C. Kovacs, G. Oakey, S. Levesque, J. Verhoef, and R. Macnab (1990b), Motion of Iberia since the Late Jurassic: Results from detailed aeromagnetic measurements in the Newfoundland Basin, *Tectonophysics*, *184*(3), 229–260.
Stapel, G. (1999), The nature of isostasy in West Iberia and its bearing on Mesozoic and Cenozoic regional tectonics, PhD thesis, 148 pp., Vrije Universiteit.
Stich, D., E. Serpelloni, F. de Lis Mancilla, and J. Morales (2006), Kinematics of the Iberia–Maghreb plate contact from seismic moment tensors and GPS observations, *Tectonophysics*, *426*(3–4), 295–317, doi:10.1016/j.tecto.2006.08.004.
Teixell, A., M.-L. Arboleya, M. Julivert, and M. Charroud (2003), Tectonic shortening and topography in the central High Atlas (Morocco), *Tectonics*, *22*(5), 1051, doi:10.1029/2002TC001460.
Terrinha, P. (1998), Structural geology and tectonic evolution of the Algarve Basin, South Portugal, PhD thesis, 430 pp., Imperial College, London.
Terrinha, P., M. Coward, and A. Ribeiro (1990), Salt tectonics in the Algarve Basin: The Loulé diapir, *Comun. Serviços Geológicos Port.*, *76*, 33–40.
Terrinha, P., C. Ribeiro, J. C. Kullberg, C. Lopes, R. Rocha, and A. Ribeiro (2002), Compressive episodes and faunal isolation during rifting, southwest Iberia, *J. Geol.*, *110*(1), 101–113.
Terrinha, P., et al. (2003), Tsunamigenic-seismogenic structures, neotectonics, sedimentary processes and slope instability on the southwest Portuguese Margin, *Mar. Geol.*, *195*(1–4), 55–73, doi:10.1016/S0025-3227(02)00682-5.
Terrinha, P., et al. (2009), Morphotectonics and strain partitioning at the Iberia–Africa plate boundary from multibeam and seismic reflection data, *Mar. Geol.*, *267*(3–4), 156–174, doi:10.1016/j.margeo.2009.09.012.
Terrinha, P., et al. (2013), A Bacia do Algarve: Estratigrafia, Paleogeografia e Tectónica, in *Geologia de Portugal, Vol. II, Geologia Meso-Cenozóica de Portugal*, edited by R. Dias et al., pp. 29–166, Cap III, Livraria Escolar Editora, Lisboa.
TGS (2005), PD00: Non-exclusive 2D survey, TGS online data zone. [Available at http://www.tgs.com/TGS/specsheets/PD-00_Spec.pdf.]
Thiebot, E., and M.-A. Gutscher (2006), The Gibraltar Arc seismogenic zone (part 1): Constraints on a shallow east dipping fault plane source for the 1755 Lisbon earthquake provided by seismic data, gravity and thermal modeling, *Tectonophysics*, *426*(1–2), 135–152, doi:10.1016/j.tecto.2006.02.024.
Torelli, L., R. Sartori, and N. Zitellini (1997), The giant chaotic body in the Atlantic Ocean off Gibraltar: New results from a deep seismic reflection survey, *Mar. Pet. Geol.*, *14*(2), 125–138, doi:10.1016/S0264-8172(96)00060-8.
Tortella, D., M. Torne, and A. Pérez-Estaún (1997), Geodynamic evolution of the eastern segment of the Azores-Gibraltar zone: The Gorringe Bank and the Gulf of Cadiz region, *Mar. Geophys. Res.*, *19*(3), 211–230.
Tugend, J., G. Manatschal, N. J. Kusznir, E. Masini, G. Mohn, and I. Thinon (2014), Formation and deformation of hyperextended rift systems: Insights from rift domain mapping in the Bay of Biscay-Pyrenees, *Tectonics*, *33*, 1239–1276, doi:10.1002/2014TC003529.
Vågnes, E., R. H. Gabrielsen, and P. Haremo (1998), Late Cretaceous-Cenozoic intraplate contractional deformation at the Norwegian continental shelf: Timing, magnitude and regional implications, *Tectonophysics*, *300*, 29–46, doi:10.1016/S0040-1951(98)00232-7.
van Hinsbergen, D. J. J., R. L. M. Vissers, and W. Spakman (2014), Origin and consequences of western Mediterranean subduction, rollback, and slab segmentation, *Tectonics*, *33*, 393–419, doi:10.1002/2013TC003349.
Vegas, R. (1980), Carboniferous subduction complex in the south Portuguese zone coeval with basement reactivation and uplift in the Iberian massif, Cuadernos do Laboratorio Xeolóxico de Laxe, vol. 1, pp. 187–200.
Vegas, R., T. Medialdea, M. Muñoz García, V. Díaz del Río, and L. Somoza (2004), Nature and tectonic setting of the Guadalquivier Bank (Gulf of Cadiz, SW Iberian Peninsula), *Rev. Soc. Geológica Esp.*, *17*(1–2), 49–60.
Vera, J. A. (1998), El Jurásico de la Cordillera Bética: Estado actual de conocimientos y problemas pendientes, *Cuad. Geol. Ibérica*, *24*, 17–42.
Vergés, J., and M. Fernàndez (2012), Tethys–Atlantic interaction along the Iberia–Africa plate boundary: The Betic–Rif orogenic system, *Tectonophysics*, *579*, 144–172, doi:10.1016/j.tecto.2012.08.032.
Ziegler, P. A. (1988), *Evolution of the Arctic-North Atlantic and the Western Tethys*, AAPG Memoir 43 ed., Amer Assn of Petroleum Geologists, Tulsa, Okla.
Zitellini, N., et al. (2001), Source of 1755 Lisbon earthquake and tsunami investigated, *Eos Trans. AGU*, *82*(26), 285–291, doi:10.1029/EO082i026p00285-01.
Zitellini, N., M. Rovere, P. Terrinha, F. Chierici, and L. Matias (2004), Neogene through Quaternary tectonic reactivation of SW Iberian passive margin, *Pure Appl. Geophys.*, *161*(3), 565–587, doi:10.1007/s00024-003-2463-4.
Zitellini, N., E. Gràcia, L. Matias, P. Terrinha, M. A. Abreu, G. DeAlteriis, J. P. Henriet, J. J. Dañobeitia, D. G. Masson, and T. Mulder (2009), The quest for the Africa–Eurasia plate boundary west of the Strait of Gibraltar, *Earth Planet. Sci. Lett.*, *280*(1–4), 13–50, doi:10.1016/j.epsl.2008.12.005.